

# Quasideuteron Mode in Odd-Odd $N=Z$ Nuclei

Inaugural-Dissertation  
zur  
Erlangung des Doktorgrades  
der Mathematisch-Naturwissenschaftlichen Fakultät  
der Universität zu Köln

vorgelegt von

**Alexander Lisetskiy**  
aus Tatarbunary, Ukraine

Köln 2002

Berichterstatter:

Prof. Dr. P. von Brentano  
Prof. Dr. J. Jolie

Tag der mündlichen Prüfung:

25. Januar 2002

*To the Grandparents of my Son*

**Facilius per partes in cognitionem totius adducimur**

*(L. Annaeus Seneca)*

*We are more easily led part by part to an understanding of the whole*  
*(Seneca the Younger)*

## Zusammenfassung

Die Untersuchung selbstkonjugierter Kerne ( $N = Z$  Kerne) in der  $pf$ -Schale ist seit den letzten Jahren eines der Hauptforschungsgebiete am Institut für Kernphysik der Universität zu Köln. Dabei konzentriert man sich auf die niederenergetische Struktur der ungerade-ungeraden  $N = Z$  Kerne  ${}^{46}_{23}\text{V}_{23}$ ,  ${}^{50}_{25}\text{Mn}_{25}$ ,  ${}^{54}_{27}\text{Co}_{27}$  und  ${}^{58}_{29}\text{Co}_{29}$ , die sehr wichtig für das konzeptionelle Verständnis der Rolle der Proton-Neutron-Wechselwirkung in Atomkernen ist. Eines der verblüffenden Ergebnisse dieser Untersuchungen war die Beobachtung sehr starker M1 Übergänge zwischen Zuständen mit  $T = 0$  und  $T = 1$ .

In dieser Arbeit wird über Betrachtungen der spezifischen Eigenschaften ungerade-ungerader  $N = Z$  Kerne berichtet. Im Rahmen des Schalenmodells wurde unter Zuhilfenahme des Konzeptes der Quasideuteronen-Konfigurationen der generierende Mechanismus für starke M1 Übergänge in ungerade-ungeraden  $N = Z$  Kernen dargelegt. Indem Formeln für  $B(M1)$ -Werte hergeleitet wurden, wurde gezeigt, dass die positive Interferenz der Spin- und Orbit-Anteile von M1 Matrixelementen für Ein-Proton-ein-Neutron  $[j_\pi \otimes j_\nu]^{J,T}$  Konfigurationen mit  $j_\pi = j_\nu = l + 1/2$  eine Hauptursache für diese Verstärkung ist. Es wurde gezeigt, dass starke M1 Übergänge in einer ganzen Klasse von Kernen im unteren Teil der  $p$ -,  $sd$ - und  $pf$ -Schale existieren, was durch die bekannten experimentellen Daten bestätigt wird. Es wird gezeigt, dass M1 Matrixelemente ein sehr effektives Werkzeug zur Identifizierung spezifischer Schalenmodell-Konfigurationen darstellen. In dieser Arbeit wurde die Beziehung zwischen Quasideuteron-Konfigurationen und Shears-Banden hergestellt, und die Relationen für die Intensitäten von  $B(M1)$  und  $B(E2)$  Werten wurden als gemeinsam für beide Phänomene erkannt. Für den Fall wohldeformierter ungerade-ungerader  $N = Z$  Kerne wurden analytische Ausdrücke für  $B(M1)$  Werte in Rahmen des Rotor-Plus-Quasideuteron-Modells hergeleitet. Die Ergebnisse der Rechnungen im vorgeschlagenen Formalismus erklären die Fragmentierung der M1 Übergangsstärken in deformierten ungerade-ungeraden  $N = Z$  Kernen und sind hilfreich beim Aufstellen interessanter Beziehungen für  $B(M1)$  Werte und helfen auch bei der Extrapolation des Bildes der Quasideuteron-M1-Mode hin zu schweren ungerade-ungeraden  $N = Z$  Kernen bis  ${}^{98}\text{In}$ . Durch die Analyse der vollen  $pf$ -Schalenmodell Rechnungen für  ${}^{46}_{23}\text{V}_{23}$  und  ${}^{50}_{25}\text{Mn}_{25}$  und den Vergleich mit dem Rotor-Plus-Quasideuteron Modell und experimentellen Daten zeigt sich, dass kollektive Eigenschaften für die niedrigliegenden Zustände in diesen Kernen massgeblich sind, und dass sich die K-Quantenzahl-Auswahlregel auf die starken M1 Übergänge auswirkt.

## Abstract

The study of the self-conjugate  $N = Z$  nuclei in the  $pf$ -shell has been one of the main topics of research performed at the Institute for Nuclear Physics at the University of Cologne in the last few years. The investigations were focused on low-energy structures of the odd-odd  $N = Z$  nuclei  ${}^{46}_{23}\text{V}_{23}$ ,  ${}^{50}_{25}\text{Mn}_{25}$ ,  ${}^{54}_{27}\text{Co}_{27}$ , and  ${}^{58}_{29}\text{Co}_{29}$  which are of great importance for the conceptual understanding of the role of proton-neutron interaction in atomic nuclei. One of the amazing findings of these studies was the observation of very strong M1 transitions between  $T = 0$  and  $T = 1$  states.

In the present work the studies of the exclusive properties of odd-odd  $N = Z$  nuclei are reported. In the framework of the nuclear shell model the generating mechanism of strong M1 transitions in odd-odd  $N = Z$  nuclei using the concept of quasideuteron configurations was revealed. By deriving analytical formulas for B(M1) values, it was shown that a positive interference of spin and orbital parts of M1 matrix elements for one-proton one-neutron  $[j_\pi \otimes j_\nu]^{J,T}$  configurations with  $j_\pi = j_\nu = l + 1/2$  is a main source for this enhancement. It was brought to view that strong M1 transitions are appropriate for a whole class of nuclei from the lower part of  $p$ ,  $sd$ , and  $pf$ -shells, what is well supported by known experimental data. Comparing the properties of low-lying states in  ${}^{54}_{27}\text{Co}_{27}$  and  ${}^{42}_{21}\text{Sc}_{21}$ , we illustrate, that M1 matrix elements are very effective tools for the identification of the specific shell model configurations and help to explore the properties of proton-neutron interaction in isovector ( $T = 1$ ) and isoscalar ( $T = 0$ ) channels. In this work, the relation between quasideuteron configurations and shears bands was established and the intensity relations for B(M1) and B(E2) values were found to be common features of both phenomena.

For the case of well deformed odd-odd  $N = Z$  nuclei in the framework of the rotor-plus-quasideuteron model, the analytical expressions for B(M1) values were derived. The results of the calculations within the proposed approach explain the fragmentation of the M1 transition strengths in deformed odd-odd  $N=Z$  nuclei. They help to establish some interesting regularities for B(M1) values as well as to extrapolate the quasideuteron picture to heavy odd-odd  $N = Z$  nuclei up to  ${}^{98}_{49}\text{In}_{49}$ . Sum rules for M1 transitions in deformed and spherical odd-odd  $N = Z$  nuclei were derived. Analyzing the full  $pf$ -shell model calculations and new experimental data for  ${}^{46}_{23}\text{V}_{23}$  and  ${}^{50}_{25}\text{Mn}_{25}$  from the perspective of the rotor-plus-quasideuteron model collective features appropriate for the low-lying states in these nuclei were identified, and K-quantum number selection rule effects on the strong M1 transitions were indicated.

# Contents

|  |           |
|--|-----------|
| <b>Zusammenfassung</b>   | <b>1</b>  |
| <b>Abstract</b>  | <b>2</b>  |
| <b>1 Introduction</b>  | <b>5</b>  |
| <b>2 Quasideuteron configurations</b>  | <b>9</b>  |
| 2.1 Basics of Nuclear Shell Model . . . . .  | 9         |
| 2.2 Two-nucleon configurations . . . . .   | 12        |
| 2.3 Quasideuteron M1 mode in odd-odd $N=Z$ nuclei . . . . .                                  | 13        |
| 2.4 Interplay between quasideuteron and spin-flip M1 modes . . . . .                         | 16        |
| 2.5 How strong can M1 transitions be? . . . . .  | 18        |
| 2.6 Quasideuteron states in $^{54}\text{Co}$ . . . . .                                       | 19        |
| 2.6.1 What can one learn about proton-neutron interaction? . . . . .                         | 21        |
| 2.6.2 M1 transitions as fine testing tools of nuclear structure . . . . .                    | 23        |
| 2.7 Quasideuteron states and magnetic rotation . . . . .                                     | 26        |
| 2.8 Intensity Relations . . . . .  | 31        |
| <b>3 Quasideuteron states with deformed core</b>   | <b>35</b> |
| 3.1 Rotor-plus-quasideuteron model . . . . .   | 35        |
| 3.2 Regularities for M1 transitions . . . . .  | 38        |
| 3.3 Spin and orbital contributions to M1 strengths . . . . .                                 | 41        |
| 3.4 Sum Rules for M1 Strengths . . . . .   | 43        |
| 3.5 Quasideuteron states in $^{46}\text{V}$ and $^{50}\text{Mn}$ . . . . .                   | 45        |
| 3.5.1 Identification of $K = 0, T = 1$ bands . . . . .                                       | 47        |
| 3.5.2 Identification of $K = 3, T = 0$ and $K = 5, T = 0$ bands . . . . .                    | 49        |
| 3.5.3 $\Delta K = 0, \Delta T = 1$ and $\Delta K = 3, \Delta T = 1$ M1 transitions . . . . . | 53        |

4

**4 Summary 55**

**List of Publication during PhD Project 58**

**Bibliography 61**



# Chapter 1

## Introduction

The concept of the atomic nucleus as a quantum system of interacting neutrons and protons introduced by W. Heisenberg [Hei32] and D. D. Iwanenko [Iwa32] is fundamental for understanding the rich and fascinating variety of nuclear phenomena. In general the theoretical description of systems of strongly interacting particles is a very complicated problem of Quantum Field Theory [Bog57]. The study of the experimentally observed properties of the atomic nuclei allows some general conclusions about the properties of nuclear forces helping to avoid the difficulties of Quantum Field Theory and develop a non-relativistic nuclear theory.

However, any nonrelativistic approximation of nuclear theory is countered with two principal problems. First, the nature of the nuclear forces is not well known. Second, the many-body problem is too difficult to be solved exactly (for  $A$  nucleons there is a system of  $2^A$  equations!); and even if exact solutions were available they would be too complex to be analyzed. Therefore, in order to make progress in understanding nuclear structure, macroscopic and microscopic models have been suggested which are based on empirical evidence and are usually adopted for describing only certain groups of phenomena. For instance, the nuclear shell model was aimed at explaining the magic numbers and the structure of atomic nuclei with few valence nucleons near a shell closure [Bar32, Els33, Els35]. In this model, the complicated motion of nucleons due to their mutual interactions is modeled by the motions of independent nucleons in a static spherical field. Immediately after the correct mathematical formulation of the model by Mayer [May49], Haxel, Jensen, and Suess [Hax49], the nuclear shell model had amazing success and was recognized as a fundamental microscopic nuclear model.

However, the observation of simple rotational like regularities in the spectra

of weakly excited states in even-even nuclei served as impressive evidence for collective nuclear phenomena. These regularities were observed in nuclei with numbers of protons and neutrons which are far from the magic numbers. These regular features were described in the unified nuclear model developed by A. Bohr and B. Mottelson [Boh53]. In this approach, the degrees of freedom of one or a few weakly bound nucleons were explicitly taken into account. These weakly bound nucleons are moving in a deformed field and thus occupy deformed orbitals which were introduced by Nilsson [Nil55]. At the same time, the collective vibrations attributed to the changes of form and orientation of the nucleus were “borrowed” from the liquid drop model. The Bohr-Mottelson model described a lot of experimental data related to the deformed nuclei and predicted some of their properties, too. Later the idea of collective nuclear properties was developed for the more general case of triaxially deformed nuclei by A. S. Davydov and G. F. Filippov [Dav58].

Shortly after the first steps in the application of the spherical shell model, it was impossible to perform shell model calculations in large configurational spaces with many active nucleons due to the technical problems. Thus, the question, whether the shell model is in principle able to describe the observed collective features of the nuclear structure remained unanswered. It was recognized that to use the shell model in the description of heavier nuclei or nuclei far from closed shells, one must come up with a reliable truncation procedure, in order to reduce the number of shell model configurations while preserving the key dynamics of the interacting nucleons. Many various truncation approaches were developed, starting with the works on the generalized seniority scheme [Ker61], SU(3) symmetry considerations [Ell58], the interacting boson approximation [Jan74, Jol75, Ari75, Ari77], the symplectic shell model [Mos84, Row85], the pseudo-SU(3) approach [Rat73, Dra83] or quasi-SU(3) scheme [Zuk95, Mar97]. Most of these approximations were primarily developed to avoid the problems of large space shell model calculations. But on the other hand, they revealed beautiful and simple paradigms allowing deep insights into the underlying physics behind the experimental data as well as behind the shell model output itself.

With recent progress in computational facilities and calculation techniques based on modern approaches like Quantum Monte Carlo Diagonalization [Ots98] and Density Matrix Renormalization Group Methods [Duk01] it becomes possible to perform exact large scale shell model calculations nowadays. Results of detailed shell model calculations carried out by Tokyo [ScM00] and Strasbourg [Car99] groups recently show, that indeed a lot of effects predicted by simple collective models and various truncation approximations really seem to be account-

able within a shell model approach.

The theoretical advances mentioned above, accompanied by intense developments of new experimental tools like the radioactive ion-beam facilities, large detector arrays or very efficient mass separator systems, have stimulated a new wave of active studies on the longstanding problem of the proton-neutron (pn) interaction and the role played by the pn degree of freedom in the formation of collective quantum phenomena such as deformation or phonon excitations [Cho91, Pet99, Fri99, Goo98, Isa97, Lan97, Len99, LiP99, OLe99, Rud96, Sat97, Sat98, ScM00, ScC99, Sko98, Sve98, Vin98]. The peculiar property of the pn inter-

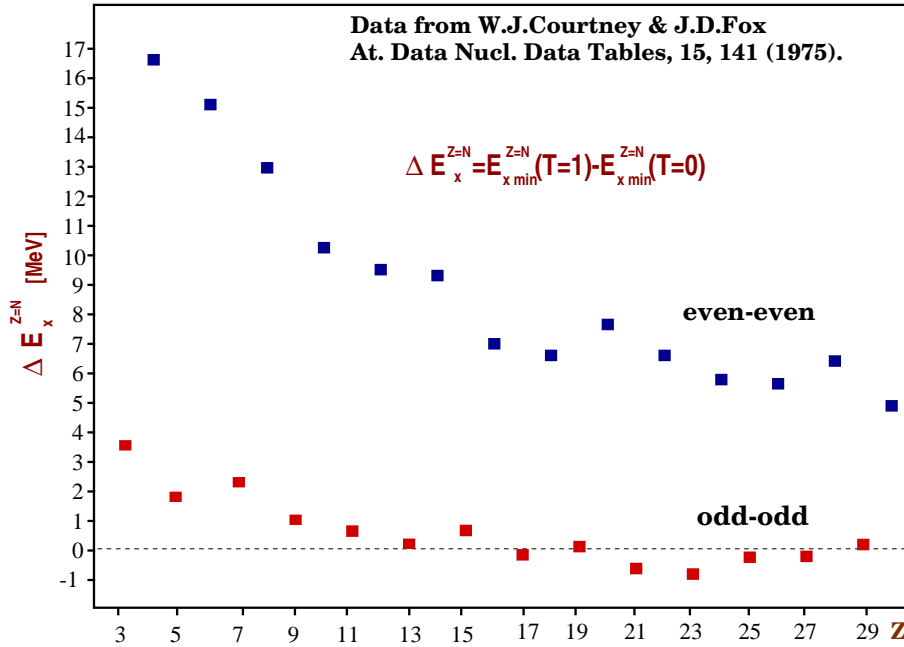


Figure 1.1: Energy difference between the lowest  $T = 1$  state and the  $0_1^+$ ,  $T = 0$  ground state in even-even nuclei (upper points) and between the  $0_1^+$ ,  $T = 1$  state and the lowest  $T = 0$  state in odd-odd nuclei (lower points).

action is, that, in contrast to proton-proton ( $T = 1, T_z = -1$ ) and neutron-neutron ( $T = 1, T_z = 1$ ) configurations, the pn pairs can either form isovector ( $T = 1, T_z = 0$ ) or isoscalar ( $T = 0, T_z = 0$ ) states. Isovector pn correlations manifest themselves in a similar fashion to like-nucleon correlations, what is evident from the properties of  $T = 1$  isobaric analogue nuclei, while the pn interaction in the isoscalar channel ( $T = 0, T_z = 0$ ) is much less understood

and currently the subject of active debate and intense studies using new theoretical and experimental tools [Goo98, Lan97, Mac00, Vog00]. The best laboratory to study the effects from the interplay between different modes of pn interaction in isovector and isoscalar channels are  $N = Z$  nuclei, while in nuclei with neutron excess (or proton excess in light  $Z > N$  nuclei) the like-nucleon  $T = 1$  pairing forces dominate. Furthermore, odd-odd  $N=Z$  nuclei are particularly interesting systems, since in these nuclei, as a consequence of a cancellation of the symmetry and pairing energies, the  $T = 0$  and  $T = 1$  states are almost degenerate (see Fig. 1.1). This creates very favorable experimental conditions to study electromagnetic transitions between low-lying  $T = 0$  and  $T = 1$  states, which is also indicated by a wealth of experimental data accumulated for light  $A < 46$  odd-odd  $N = Z$  nuclei. One of the interesting phenomena related to the interplay of  $T = 0$  and  $T = 1$  states, which we tried to attract the attention of the nuclear physics community to in a series of our papers [LiP99, LiL01, BrE00, BrB00, BrM01, BrE01, LiG01, ScM00, ScC99], is the occurrence of very strong  $\Delta T = 1$  M1 transitions in some odd-odd  $N=Z$  nuclei.

The present work is aimed at explaining the origin of these extraordinary strong M1 transitions introducing the simple concept of quasideuteron configurations within the framework of the spherical shell model and the unified model.

The studies presented in Chapter 2 show, which information on the pn interaction can be obtained using M1 transitions, what magnetic rotation has in common with the quasideuteron mode, what the results of the interplay of the quasideuteron mode with the spin-flip mode are, what the sum rules for M1 strengths generated by pn pair are, and how strong M1 transitions are permissible to be in atomic nuclei.

In Chapter 3 it is demonstrated, how quasideuteron configurations behave in the presence of quadrupole deformation, which properties of deformed nuclei they can help to reveal, what the regularities for M1 transitions are, how the concept of quasideuteron configurations can serve as a guideline for the large scale shell model and experimental studies of atomic nuclei in the pf-shell as well as exotic proton-rich nuclei in the region up to  $^{98}\text{In}$ , which actually is declared to be a region of high interest of modern nuclear structure physics.

# Chapter 2

## Quasideuteron configurations with spherical core

### 2.1 Basics of Nuclear Shell Model

The basic assumption in the nuclear shell model is, that to first order, each nucleon is moving in an independent way in an average field. This suggests, that the total Hamiltonian  $H_0$  of a system of  $A$  nucleons can be written as a sum of single particle Hamiltonian operators:

$$H = \sum_{i=1}^A h_i, \quad (2.1)$$

where  $h_i = T_i + U_i$ , i.e. each  $h_i$  is a sum of the kinetic  $T_i$  and the average field potential energy  $U_i$ . Then, the single particle wave functions  $\varphi_a(i)$  are solutions to the Schrödinger one body equation

$$h_i \varphi_a(i) = \varepsilon_a \varphi_a(i), \quad (2.2)$$

where the multi-index  $i$  denotes single particle spatial, spin and isospin coordinates  $i \equiv \{\mathbf{r}_i, \sigma_i, \tau_i\}$ ,  $a$  denotes the set of single particle quantum numbers and  $\varepsilon_a$  is the single particle energy. The total wave function of an  $A$ -body system is a solution to the Schrödinger equation with total hamiltonian  $H$  (2.1) and is represented as an antisymmetrized product (Slater determinant) of single particle wave

functions:

$$\Psi_{a_1, \dots, a_A}(i = 1, \dots, A) = \frac{1}{\sqrt{A!}} \begin{vmatrix} \varphi_{a_1}(1) & \varphi_{a_1}(2) & \cdots & \varphi_{a_1}(A) \\ \varphi_{a_2}(1) & \varphi_{a_2}(2) & \cdots & \varphi_{a_2}(A) \\ \cdots & \cdots & \cdots & \cdots \\ \varphi_{a_A}(1) & \varphi_{a_A}(2) & \cdots & \varphi_{a_A}(A) \end{vmatrix}. \quad (2.3)$$

The set of single particle quantum numbers  $a_i$  depends on the form of the single particle Hamiltonian  $h_i$ . While the form of the single particle kinetic energy operator is well defined, the average potential field can be chosen in different ways. However, because of the short range nature of nuclear forces, this potential well must have sharp boundaries, which are related to those of the matter distribution in the nucleus. For practical reasons such wells should also be amenable to calculations. The potential of the spherical harmonic oscillator

$$\frac{m_i \omega^2 r_i^2}{2}$$

satisfies these conditions and is usually used as basic ingredient for the total single particle Hamiltonian. In order to reproduce higher magic numbers a phenomenological spin-orbit potential ( $\mathbf{l}_i \cdot \mathbf{s}_i$ ) [May49, Hax49] and the orbital-orbital  $\mathbf{l}_i^2$  [Nil55] term had been added to the harmonic oscillator:

$$U(r_i) = \frac{m_i \omega^2 r_i^2}{2} - C \mathbf{l}_i \cdot \mathbf{s}_i - D \mathbf{l}_i^2. \quad (2.4)$$

The constant  $C$  characterizes the strength of the spin-orbit coupling and the parameter  $D$  simulates the deviation of the oscillator potential from a more realistic one. Both parameters are always positive for the oscillator potential.

The single particle Hamiltonian (2.4) and corresponding single particle wave functions with quantum numbers  $Nlj$  constitute the building blocks of the nuclear shell model. The single particle level scheme for the Hamiltonian above (see Fig.2.1) is of great importance for establishing the shell closures and determination of the dominant single  $j$ -orbitals for any atomic nucleus and thus for the qualitative prediction of the structure of the nuclear states. The residual interaction, i.e. the interaction between nucleons, which is not included in the average field and has a predominant two-body character can strongly mix configurations with various  $j$ -orbitals. Choosing the appropriate form of the residual interaction is one of the fundamental problems in nuclear structure physics. Detailed descriptions of this problem and possible ways of its solution are described in many shell model books (see for example [Hey94, Bru77]).

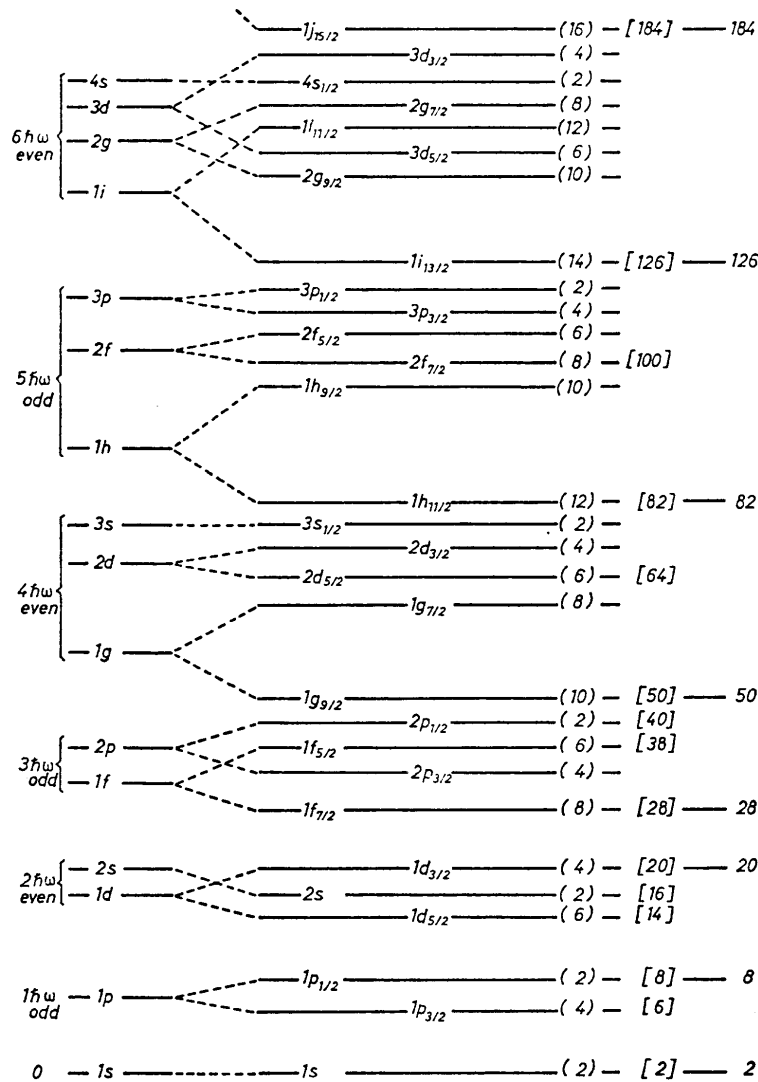


Figure 2.1: The single-particle level sequence for a Hamiltonian consisting of a central harmonic oscillator potential plus a spin-orbit splitting. The number of particles in each shell is shown, as well as the cumulative number of particles [May55].

However, there are cases in which some of the observables are not very sensitive to the residual interaction. Thus, using the average field approximation, one can already conclude about the structure of the observed states. Some of these cases are considered in the next sections.

## 2.2 Two-nucleon configurations

In the description of the full Hamiltonian for a nucleus formed by a closed shell system ( $J^\pi = 0^+$  inert core with  $H_c$ ) and two extra valence nucleons with the single-particle Hamiltonian  $h_0(i)$  the total wave functions  $\Psi_{j_1, j_2, JM}(1, 2)$  are eigenfunctions of

$$H = H_c + h_0(1) + h_0(2), \quad (2.5)$$

with eigenvalues  $E_{c,1,2} = E_c + \varepsilon_1 + \varepsilon_2$ .  $j_i$  and  $J$  denote single particle angular momentum and total angular momentum, respectively. The wave function of such a system is well established for any possible value  $J$  of the total angular momentum:  $|j_1 - j_2| \leq J \leq j_1 + j_2$ . Without a two body interaction  $V(1, 2)$  in Eq.(2.5) all the states with different values of spin  $J$  will be degenerated. A residual interaction  $V(1, 2)$  will split the degeneracy in  $J$  for the  $[j_1 \times j_2]_J$  multiplet of states, but will not affect the structure of the states and subsequently will not influence the matrix elements of electromagnetic transition operators.

In the case of two nucleon configurations, the concept of isobaric spin (isospin) is most illustrative. Isospin had been introduced to express the fact that forces between a pair of nucleons in a given state do not strongly depend on the nature of the nucleons (i.e. if they are protons or neutrons or one of each). If the pair of nucleons is in an antisymmetric state, the Pauli principle causes no restrictions; such a state is available to all three types of nucleon pairs, and strict charge independence of the forces would ensure that the three resulting physical systems have identical energies as well as identical descriptions in space and spin. The Pauli principle does not allow two identical nucleons to be in an overall symmetric state; such a state would only be available to a proton-neutron pair and have no counterpart in the other systems.

The isospin description of this situation attributes an extra quantum number to nucleons, the isospin  $t$  of magnitude  $\frac{1}{2}$ . While this does not correspond to any physical angular momentum, it possesses all the algebraic properties of a spin. Any state of a nucleus will be characterized by a total isobaric spin quantum number  $T$  and a value  $T_z$  of the third component in the isospin space. The latter is



simply half the difference between the neutron number  $N$  and the proton number  $Z$  and is always a good quantum number. Corresponding states which differ only in their  $T_z$  value therefore belong to different systems of the same mass and are said to form an isobaric multiplet. Since  $\mathbf{T}$  behaves like an angular momentum, one has the usual rule that  $T_z$  cannot exceed  $T$ . Thus  $T = 0$  are singlets, existing only in systems with  $N = Z$ ,  $T = 1/2$  states are doublets in odd mass nuclei (like the neutron and proton with  $t_z = \pm\frac{1}{2}$  respectively) and so on. Today there is experimental data available for more than 290  $T = 1/2$  analog doublets, 110  $T = 1$  triplets, 26  $T = 3/2$  quartets, and 6  $T = 2$  analog quintets [Bri98]. The pair of nucleons mentioned above, which forms three degenerate states antisymmetric in space-spin, would be described as a  $T = 1$  system; that is, an isospin triplet with  $T_z = +1$  (two neutrons),  $T_z = 0$  (neutron-proton) and  $T_z = -1$  (two protons). When such a nucleon pair couples to the  $T = 0, T_z = 0$  even-even core they will also form an isospin triplet.

However a p-n pair can also exist in a  $T = 0$  state for which there is no need for equality with the  $T = 1$  n-p, p-p and n-n forces. The properties of the proton-neutron interaction in this  $T = 0$  state is one of the most active areas of current research in nuclear structure physics. Effects from the interplay between different modes of the proton-neutron interaction in isovector ( $T = 1$ ) and isoscalar ( $T = 0$ ) channels can be studied in  $N = Z$  nuclei, while in nuclei with neutron excess (or proton excess in light  $N \neq Z$  nuclei) the neutron-neutron (proton-proton)  $T = 1$  pairing forces dominate. The odd-odd  $N = Z$  nuclei are particularly interesting objects since the  $T = 0$  and  $T = 1$  states are almost degenerate as a consequence of a cancellation of the symmetry and pairing energies [BrE00, Mac00, Vog00] in these nuclei. The contemporary advances in experimental techniques enable one to obtain spectroscopic data on the nuclear structure of heavy  $N = Z$  nuclei nowadays and hopefully give some clues resolving the problem of proton-neutron pairing correlations. In the light of this interest, the low-spin structure of odd-odd  $N = Z$  nuclei  $^{46}\text{V}$  [BrM01, Fri99, Fri00, Sch00],  $^{50}\text{Mn}$  [BrB00, ScM00],  $^{54}\text{Co}$  [BrE00, ScC99] and  $^{58}\text{Cu}$  [BrM01, Sch00] was studied in Cologne recently. In the next sections the most interesting findings of our studies are stressed.

## 2.3 Quasideuteron M1 mode in odd-odd $N=Z$ nuclei

In order to study medium heavy odd-odd  $N = Z$  nuclei, the experimental data available for all odd-odd  $N = Z$  nuclei has been analyzed with the aim to find common nuclear structure features appropriate for this class of nuclei (except the

well known fact of degeneracy of  $T = 0$  and  $T = 1$  states). However, very striking differences between the spectra as well as the electromagnetic transition strengths have been found for the odd-odd  $N = Z$  nuclei from different parts of the same N-oscillator shell. While spectra, magnetic dipole moments, E2 transition strengths for the odd-odd  $N = Z$  nuclei from  $p-$ ,  $sd-$ , and  $pf$ -shells were intensely discussed, analyzed and interpreted in the frames of various approaches, the occurrence of very strong M1 transitions and their origin has been overlooked in a bulk of papers and books despite the known experimental data. Thus, analyzing the data, it was noted that some of the odd-odd  $N = Z$  nuclei, namely  ${}^6\text{Li}$ ,  ${}^{18}\text{F}$  and  ${}^{42}\text{Sc}$  exhibit very strong isovector M1 transitions between the yrast states with quantum numbers  $J^\pi = 0_1^+, T = 1$  and  $J^\pi = 1_1^+, T = 0$  (see Table 2.1) while the transitions from  $J^\pi = 0_1^+, T = 1$  to other  $J^\pi = 1_i^+, T = 0$  states are negligible weak. In other nuclei, for example like in  ${}^{22}\text{Na}$ , the large M1 strength is distributed among two or three low-lying  $J^\pi = 1^+$  states. Finally the odd-odd  $N = Z$  nuclei  ${}^{14}\text{N}$ ,  ${}^{30}\text{P}$ ,  ${}^{34}\text{Cl}$ ,  ${}^{38}\text{K}$  have considerably weaker  $0_1^+, T = 1 \rightarrow 1_1^+, T = 0$  transitions, in some cases with almost vanishing M1 strengths.

Attempting to understand this interesting phenomena [LiP99], an odd-odd  $N = Z$  nucleus was considered as an inert  $J_T^\pi = 0_0^+$  even-even  $N=Z$  core coupled to two valence nucleons, one proton and one neutron in the same shell model orbital with quantum numbers  $(nlj)$ .

The two nucleon  $[\pi j \times \nu j]_{M, T_z=0}^{J, T}$  multiplet of states splits into two sequences with different isospin symmetry:  $T = 0$ , (odd spin values  $J = 1, 3, \dots, 2j$ ) and  $T = 1$  (even spin values  $J = 0, 2, \dots, 2j - 1$ ). In the lowest states of the deuteron, the bound  $J_T^\pi = 1^+, T = 0$  ground state and the unbound  $J_T^\pi = 0^+, T = 1$  resonance, both nucleons occupy the  $1s_{1/2}$  orbital, i.e. the one with  $j = l + 1/2$  and  $l = 0$ .

In generalization of the deuteron case the wave functions  $[[\pi j \times \nu j]; J, T\rangle$  were denoted as *quasi-deuteron configurations* (QDC).

To calculate M1 matrix elements one starts with a nuclear magnetic dipole operator, which is the sum of proton and neutron one-body terms for spin and orbital contributions:

$$\mathbf{T}(M1) = \sqrt{\frac{3}{4\pi}} \left( \sum_{i=1}^Z [g_p^l \mathbf{I}_i^p + g_p^s \mathbf{S}_i^p] + \sum_{i=1}^N [g_n^l \mathbf{I}_i^n + g_n^s \mathbf{S}_i^n] \right) \mu_N, \quad (2.6)$$

where  $g_\rho^l$  and  $g_\rho^s$  are the orbital and spin  $g$ -factors and  $\mathbf{I}_i^\rho, \mathbf{S}_i^\rho$  are the single particle orbital angular momentum and spin operators for  $\rho \in \{p, n\}$  and  $\mu_N = e\hbar/2M_p c$  represents the nuclear magneton. The bare values of  $g$ -factors are:  $g_p^{l, \text{bare}} = 1$ ,

$g_n^{l,\text{bare}} = 0$ ,  $g_p^{s,\text{bare}} = 5.58$ , and  $g_n^{s,\text{bare}} = -3.82$ .

A  $\Delta T = 1$  isovector M1 transition, for instance between the  $0^+$ ,  $T = 1$  and  $1^+$ ,  $T = 0$  yrast states in odd-odd  $N = Z$  nuclei, is generated by the isovector (IV) part of the M1 transition operator

$$\mathbf{T}_{IV}(M1) = \sqrt{\frac{3}{4\pi}} \left[ \frac{g_p^l - g_n^l}{2} (\mathbf{L}_p - \mathbf{L}_n) + \frac{g_p^s - g_n^s}{2} (\mathbf{S}_p - \mathbf{S}_n) \right] \frac{\mu_N}{\hbar}, \quad (2.7)$$

where  $\mathbf{L}_\rho = \sum_i \mathbf{l}_i^\rho$  and  $\mathbf{S}_\rho = \sum_i \mathbf{s}_i^\rho$  with  $\rho = p, n$ . This is a consequence of the tensor properties of the M1 transition operator in isospin space. The states with isospin quantum number  $T = 0$  and  $T = 1$  and spins  $J$  and  $J + 1$  are connected by M1 transitions. The  $B(M1)$  values for these transitions are given by simple analytical formulae [LiP99]:

$$B(M1; J \rightarrow J + 1) = \frac{3}{4\pi} \frac{J + 1}{2J + 1} \left( j + 1 + \frac{J}{2} \right) \left( j - \frac{J}{2} \right) \left( g_{IV}^j \right)^2 \mu_N^2, \quad (2.8)$$

$$\text{where } g_{IV}^j = g_p^j - g_n^j = \frac{l + \alpha_q \cdot 4.706}{j} \quad \text{for } j = l + 1/2 \quad (2.9)$$

$$\text{and } g_{IV}^j = \frac{l + 1 - \alpha_q \cdot 4.706}{j + 1} \quad \text{for } j = l - 1/2, \quad (2.10)$$

where the values of the orbital  $g$ -factors are taken to be bare ( $g_p^{l,\text{bare}} = 1$ ,  $g_n^{l,\text{bare}} = 0$ ) and  $\alpha_q$  is a quenching factor for the bare spin  $g$ -factors ( $g_p^{s,\text{bare}} = 5.58$  and  $g_n^{s,\text{bare}} = -3.82$ ). Looking at Eqs. (2.9) and (2.10) one can immediately see the origin of the phenomena. The positive interference of large spin and orbital parts of the isovector  $\Delta T=1$  M1 reduced matrix elements in the  $j = l + 1/2$  case (see Eq. (2.9)) causes a strong enhancement of  $\Delta T = 1$  M1 transitions between quasideuteron states with  $j = l + 1/2$  in odd-odd  $N = Z$  nuclei. Actually the strongest known  $0^+ \rightarrow 1^+$  M1 transitions between low-lying nuclear states are observed in spherical odd-odd  $N = Z$  nuclei in the lower part of the  $p$ -,  $sd$ - and  $pf$ -shells, where the  $j = l + 1/2$  orbitals play a dominant role. On the contrary, for the odd-odd  $N = Z$  nuclei in the upper part of the  $p$ - and  $sd$ -shells, the  $0^+ \rightarrow 1^+$  M1 transitions are strongly suppressed due to the destructive interference of spin and orbital parts of the M1 matrix elements for one-proton-one-neutron configurations in a single  $j = l - 1/2$  orbital (see Eq. (2.10)). The  $B(M1)$  values calculated from Eq. (2.8) assuming reasonable single particle orbitals are given in Table 2.1 together with the corresponding experimental  $B(M1)$  values.

Table 2.1: *Experimental and calculated B(M1) values for odd-odd  $N = Z$  nuclei. In the columns labeled by “Th1” and “Th2” the results of calculations using Eqs. (2.8) and (2.14), respectively, are shown. The free spin g-factors were used for calculations.*

| Nucleus                 | orbital<br>$nlj$ | $E_x^{\text{exp}}$ [MeV] |         | $B(M1; 0_1^+ \rightarrow 1_1^+)[\mu_N^2]$ |       |       |
|-------------------------|------------------|--------------------------|---------|---|-------|-------|
|                         |                  | $0_1^+$                  | $1_1^+$ | Expt.                                     | Th1   | Th2   |
| ${}^2_1\text{H}$        | $1s_{1/2}$       | 2.400                    | 0       | -   | 15.86 | 15.86 |
| ${}^6_3\text{Li}$       | $1p_{3/2}$       | 3.562                    | 0       | 15.4(4)                                   | 12.96 | 15.77 |
| ${}^{18}_9\text{F}$     | $1d_{5/2}$       | 1.041                    | 0       | 20(4)                                     | 15.18 | 18.41 |
| ${}^{42}_{21}\text{Sc}$ | $1f_{7/2}$       | 0                        | 0.611   | 11(4)                                     | 18.23 | 21.85 |
| ${}^{34}_{17}\text{Cl}$ | $1d_{3/2}$       | 0                        | 0.461   | 0.23(2)                                   | 0.42  |       |
| ${}^{38}_{19}\text{K}$  | $1d_{3/2}$       | 0.130                    | 0.460   | 0.47(4)                                   | 0.42  |       |

## 2.4 Interplay between quasideuteron and spin-flip M1 modes

Comparing large experimental and theoretical B(M1) values for  ${}^6_3\text{Li}$  and  ${}^{18}_9\text{F}$ , it can be seen that the main contribution ( $\sim 85\%$ ) to the M1 strength originates from the quasideuteron configurations with  $j = l + 1/2$ . It is interesting to see, in which way large M1 matrix elements can be generated by other mechanisms different from the quasideuteron case. Analyzing single-particle M1 matrix elements, it is easy to recognize that the additional source of the enhancement of  $0_1^+ \rightarrow 1_1^+$  M1 transition strength can be an admixture of the  $[(j = l + 1/2) \times (j = l - 1/2)]$ ;  $J = 1, T = 0$  state to the quasideuteron  $[(j = l + 1/2) \times (j = l + 1/2)]$ ;  $J = 1, T = 0$  state. The corresponding isovector M1 matrix element generated by this spin-flip component is

$$\langle [j]^2; 0^+ \| T(M1) \| [j \times j']; 1^+ \rangle = \sqrt{\frac{3}{4\pi}} \sqrt{\frac{2l}{2l+1}} \left( \frac{1}{2} - \alpha_q 4.706 \right), \quad (2.11)$$

for  $j = l + 1/2$  and  $j' = l - 1/2$ . In the case of the  $0^+$  state formed by the proton and neutron in the  $j' = l - 1/2$  state, one gets a slightly different expression:

$$\langle [j']^2; 0^+ \| T(M1) \| [j \times j']; 1^+ \rangle = \sqrt{\frac{3}{4\pi}} \sqrt{\frac{2l+2}{2l+1}} \left( \frac{1}{2} - \alpha_q 4.706 \right). \quad (2.12)$$

Using Eqs. (2.11) and (2.12) one can show, that the M1 transition strength related to the isovector part of spin-flip mechanism is considerably smaller than the

## 2.4. INTERPLAY BETWEEN QUASIDEUTERON AND SPIN-FLIP M1 MODES<sup>17</sup>

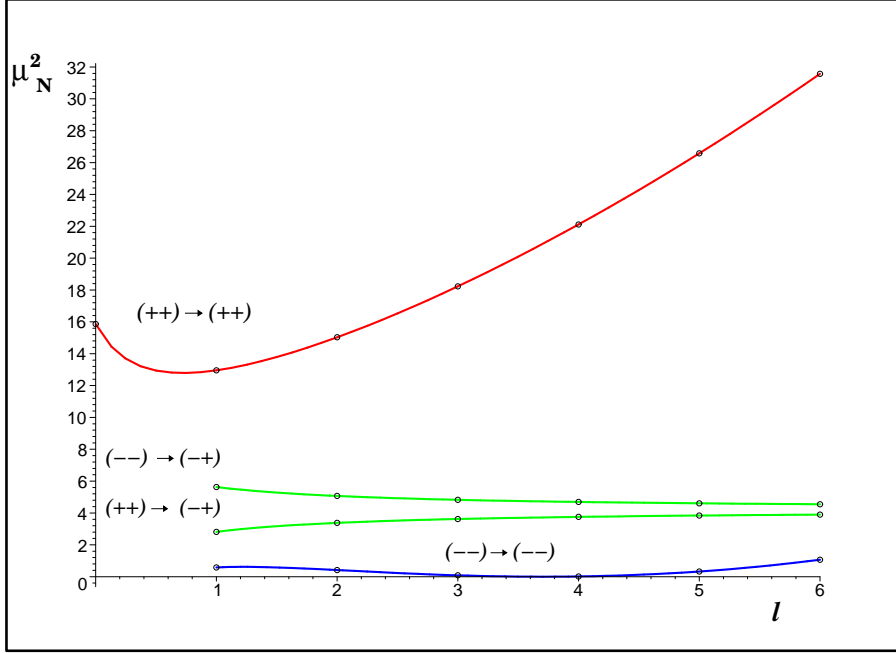


Figure 2.2: The comparison of  $B(M1; 0^+ \rightarrow 1^+)$  values for different possible one-proton-one-neutron configurations for the  $0^+$  and  $1^+$  states. For the two nucleon configurations  $(j \times j')$  the notation  $(ik)$  is used, where  $i, k = +$  for the  $j = l + 1/2$  orbital and  $i, k = -$  for  $j = l - 1/2$  orbital. For the quasideuteron  $((++) \rightarrow ((++))$  and  $((--)) \rightarrow ((--))$  cases, Eq. (2.8) was used. To calculate the spin-flip  $((++) \rightarrow ((-+))$  and  $((--)) \rightarrow ((-+))$  M1 transitions Eqs. (2.11) and (2.12), respectively, were used.

one for the quasideuteron configurations with  $j = l + 1/2$ , which is depicted in Fig. 2.2. It must be noted, that this result is important not only for odd-odd nuclei, where the one-proton-one-neutron configurations are pronounced, but also for the even-even nuclei where more complicated multi-nucleon configurations are involved.

Furthermore it is noteworthy, that positive interference of the spin-flip and quasideuteron parts of M1 matrix elements can result in  $B(M1)$  values larger than the ones yielded by Eq. (2.8). For that purpose, the  $0^+, T = 1$  state with the following structure is considered:

$$|0^+, T = 1\rangle = \left| [(j = l + 1/2)^2]_{T_z=0}^{T=1}; J = 0 \right\rangle.$$

The  $1^+, T = 0$  state is supposed to be a superposition of quasideuteron and spin-

flip components:

$$|1^+, T = 1\rangle = \beta \left| [j^2]_{T_z=0}^{T=0}; J = 1 \right\rangle + \sqrt{1 - \beta^2} \left| [j \times j']_{T_z=0}^{T=0}; J = 1 \right\rangle, \quad (2.13)$$

where  $j = l + 1/2$  and  $j' = l - 1/2$ . Then it is easy to maximize the  $B(M1, 0^+ \rightarrow 1^+)$  value varying the parameter  $\beta$ . It was found, that the maximum value for this case is the sum of  $B(M1)$  values given by Eqs. (2.8) and (2.11):

$$B_{l+\frac{1}{2}}^{\max}(M1) = \frac{3}{4\pi} \left[ \frac{2l+3}{2l+1} (l + \alpha_q 4.706)^2 + \frac{2l}{2l+1} \left( \frac{1}{2} - \alpha_q 4.706 \right)^2 \right] \mu_N^2. \quad (2.14)$$

In other words, Eq. (2.14) represents the M1 sum rule for the two-nucleon  $|0^+, T = 1\rangle = \left| [(j = l + 1/2)^2]_{T_z=0}^{T=1}; J = 0 \right\rangle$  state:

$$B_{j=l+1/2}^{\max}(M1; 0^+ \rightarrow 1^+) = \sum_i B(M1; 0^+ \rightarrow 1_i^+). \quad (2.15)$$

Using Eq. (2.14) the  $B^{\max}(M1; 0^+ \rightarrow 1^+)$  values with bare  $g$ -factors ( $\alpha_q = 1$ ) were calculated for different shells. The results of these calculations are given in the last column of Table (2.1). It is interesting to note, that for both  ${}^6_3\text{Li}$  and  ${}^{18}_9\text{F}$  the calculated maximum  $B(M1)$  values in the case above are very close to the corresponding experimental data.

## 2.5 How strong can M1 transitions be?

Actually one can estimate the maximum possible M1 strength which can be concentrated in one  $0^+ \rightarrow 1^+$  transition for any harmonic oscillator shell. As a most simple example, the case of one proton and one neutron in the  $1p$ -shell is considered. In this case the  $0^+, T = 1$  state has two components:

$$|0^+, T = 1\rangle = \alpha \left| [p_{3/2}^2]_{T_z=0}^{T=1}; J = 0 \right\rangle + \sqrt{1 - \alpha^2} \left| [p_{1/2}^2]_{T_z=0}^{T=1}; J = 0 \right\rangle, \quad (2.16)$$

and the  $1^+, T = 0$  state is a combination of three states:

$$|1^+, T = 1\rangle = \beta_1 \left| [p_{3/2}^2]_{T_z=0}^{T=0}; J = 1 \right\rangle + \beta_2 \left| [p_{1/2}^2]_{T_z=0}^{T=0}; J = 1 \right\rangle + \quad (2.17)$$

$$\sqrt{1 - \beta_1^2 - \beta_2^2} \left| [p_{1/2} \times p_{3/2}]_{T_z=0}^{T=0}; J = 1 \right\rangle.$$

Thus there are three variables:  $\alpha$ ,  $\beta_1$  and  $\beta_2$ . Using Eqs. (2.8), (2.11) and (2.12) the expression for the  $B(\text{M1})$  values can be written as a function of the three variables above and can be maximized. One finds, that the  $B(\text{M1}; 0^+ \rightarrow 1^+)$  value achieves its maximum of  $17.21 \mu_N^2$  at  $\alpha_{\text{max}} = 0.940$ ,  $\beta_{1,\text{max}} = 0.816$  and  $\beta_{2,\text{max}} = -0.063$ . Thus, it is shown in a simple way how the interplay between different mechanisms can enhance the M1 strength to its maximum value. But in any case, one can see, that the quasideuteron configurations with  $j = l + 1/2$  play the key role in the enhancement of M1 transitions.

A more detailed analysis of M1 transitions for the particular odd-odd  $N = Z$  nuclei has been presented in a recent paper [LiP99]. It was also shown, that  $B(\text{M1})$  strengths in odd-odd  $N = Z$  nuclei are related to the magnetic moments of neighboring odd- $N$  and odd- $Z$  nuclei in a very simple way. The derived relation was found to be rather useful for the estimation of M1 strengths in odd-odd  $N = Z$  nuclei using known experimental magnetic dipole moments in odd- $A$  nuclei.

## 2.6 Quasideuteron states in $^{54}\text{Co}$

The low-spin structure of the odd-odd  $N = Z$  nucleus  $^{54}\text{Co}$  was recently investigated in Cologne [ScC99]. The hitherto known (see, for instance [Rud98]) low spin level scheme of  $^{54}\text{Co}$  has considerably been enlarged and the characteristics of some low-lying states have been established. This section focuses on the results of the work [ScC99] where a very good example of quasideuteron states has been found.

To understand the structure of the low-lying states observed in  $^{54}\text{Co}$ , spherical shell-model calculations with the residual Surface Delta Interaction (SDI) [Pla66, Bru77] were performed in two different configurational spaces considering  $^{56}\text{Ni}$  as an inert core [ScC99]. Here, the simplest case is analyzed, where only the proton  $\pi f_{7/2}$  and neutron  $\nu f_{7/2}$  valence orbitals were taken into account. It is well known, that the  $f_{7/2}$  orbital is well separated from the lower lying sd-shell (5 MeV) and the next higher lying orbital is  $p_{3/2}$  (4MeV). Thus, in the case of  $^{54}\text{Co}$  (27 protons and 27 neutrons) the valence orbital  $f_{7/2}$  is occupied with one proton hole and one neutron hole below the inert  $^{56}\text{Ni}$  core. Within this limited configurational space proton and neutron holes couple to the even-spin ( $J = 0, 2, 4, 6$ )  $T = 1$  multiplet and odd-spin ( $J = 1, 3, 5, 7$ )  $T = 0$  multiplet. The residual nucleon-nucleon SDI has the following form

$$V_{\text{SDI}}(1, 2) = -4\pi A'_T \delta(\Omega_{12}) \delta(r_1 - R) \delta(r_2 - R) + B'(\tau_1 \cdot \tau_2), \quad (2.18)$$

where  $\Omega_{12}$  is the angle between the interacting particles,  $R = 1.2A^{1/3}$  fm is the nuclear radius,  $A'_{T=0}$  and  $A'_{T=1}$  are the strength constants of the SDI for the two possible isospin quantum numbers. The parameter  $B'$  adjusts the shift of the  $T = 0$  and  $T = 1$  centroids of level energies and is related to the isospin monopole part of the residual two-body interaction. The SDI parameters  $A'_{T=0}$  and  $A'_{T=1}$  regulate the splitting of the odd-spin and even spin states, respectively. The SDI is a very simple interaction from the mathematical point of view. In the considered case of a single- $j$ -orbital, one has only diagonal matrix elements of the SDI, which determine the splitting of the states with different spin values  $J$  within the  $T = 1$  and  $T = 0$  multiplets, respectively:

$$E_{T=1}(J, j^2) = -A_{T=1} \frac{(2j+1)^2}{2} \begin{pmatrix} j & j & J \\ \frac{1}{2} & -\frac{1}{2} & 0 \end{pmatrix}^2 + B; \quad (2.19)$$

$$E_{T=0}(J, j^2) = -A_{T=0} \frac{(2j+1)^2}{2} \begin{pmatrix} j & j & J \\ \frac{1}{2} & -\frac{1}{2} & 0 \end{pmatrix}^2 \left[ 1 + \frac{(2j+1)^2}{J(J+1)} \right] - 3B, \quad (2.20)$$

where  $\begin{pmatrix} j & j & J \\ \frac{1}{2} & -\frac{1}{2} & 0 \end{pmatrix}$  is the 3- $j$  symbol. Using three parameters  $A_{T=1}$ ,  $A_{T=0}$  and  $B$ <sup>1</sup> one can fit experimental spectra (see Fig. 2.3). It was found that the optimal values of the interaction parameters for the considered case are:  $A_{T=1} = A_{T=0} = 0.75$  MeV and  $B = 0.11$  MeV. Using an interaction as simple as the SDI and the  $f_{7/2}$  model space, one can reproduce the excitation energies of the yrast states with  $J < 7$ . The excitation energy of the  $7_1^+$  state is not obtained satisfactorily. This problem remains also for the enlarged configurational space which, aside from the  $f_{7/2}$  configuration, also takes the one-nucleon excitations to the  $p_{3/2}$  orbital into account. The underestimation of the two-body matrix element for the maximum spin value  $J = 2j$  by the SDI is known to be a general problem for any  $j$ -orbital. The interaction in this channel can be enhanced using an additional factor  $1 + \delta_{J,2j}$  for two-body matrix elements given by Eq. (2.20). Therefore, the  $\langle J^\pi = 7^+ | V_{\text{SDI}} | J^\pi = 7^+ \rangle_{B=0}$  matrix element for the  $f_{7/2}$  shell was replaced by  $2 \langle J^\pi = 7^+ | V_{\text{SDI}} | J^\pi = 7^+ \rangle_{B=0}$  in order to reproduce the experimentally observed 0.197 MeV excitation energy of the  $J^\pi = 7^+$  state (see Fig. 2.3).

However, it is still remarkable, that the SDI qualitatively reproduces the experimental behavior of the energies as a function of spin  $J$  for the  $T = 0$  multiplet

---

<sup>1</sup>The fitted interaction parameters  $A_T$  are connected to  $A'_T$  by the following expression:  $A_T = A'_T \langle \delta(r_1 - R) \delta(r_2 - R) \rangle$ , where the radial matrix element  $\langle \delta(r_1 - R) \delta(r_2 - R) \rangle$  is supposed to be independent from the single particle states involved (see [Bru77] for details). The same is valid for the parameters  $B$  and  $B'$ .



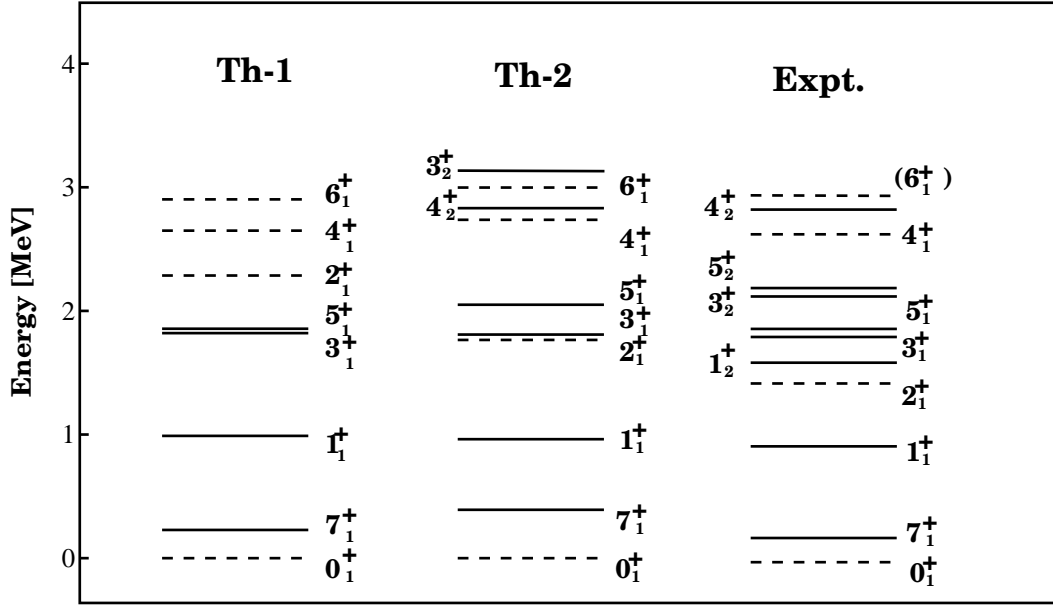


Figure 2.3: Comparison of calculated and experimental spectra of the  $J^\pi = 0^+ - 7^+$  states in  $^{54}\text{Co}$ . Th-1 and Th-2 label the calculations within  $(f_{7/2})$  and  $(f_{7/2}, p_{3/2})$  configurational spaces, respectively. The states with isospin quantum number  $T = 1$  are plotted with dashed lines and  $T = 0$  with solid lines.

(known as “parabolic rule” [Hey94]) and for the  $T = 1$  sequence of states (see Fig.2.4).

### 2.6.1 What can one learn about proton-neutron interaction ?

Basing on this result some conclusions can be made about the proton-neutron residual interaction in different isospin ( $T = 0$  and  $T = 1$ ) channels. As mentioned before, the SDI parameters  $A_{T=0}$  and  $A_{T=1}$  are equal. However, this equality does not automatically mean, that  $T = 0$  and  $T = 1$  interaction strengths are equal. There is an extra parameter  $B$  (see Eqs. (2.19) and (2.20)) which can be attributed to the additional long-range monopole part of the residual interaction. As it can be seen from Eqs. (2.19) and (2.20), this part destructively acts on the energies of  $T = 1$  states but substantially enhances the  $T=0$  two body matrix elements. As a characteristic of the interaction, one can use the average two-body

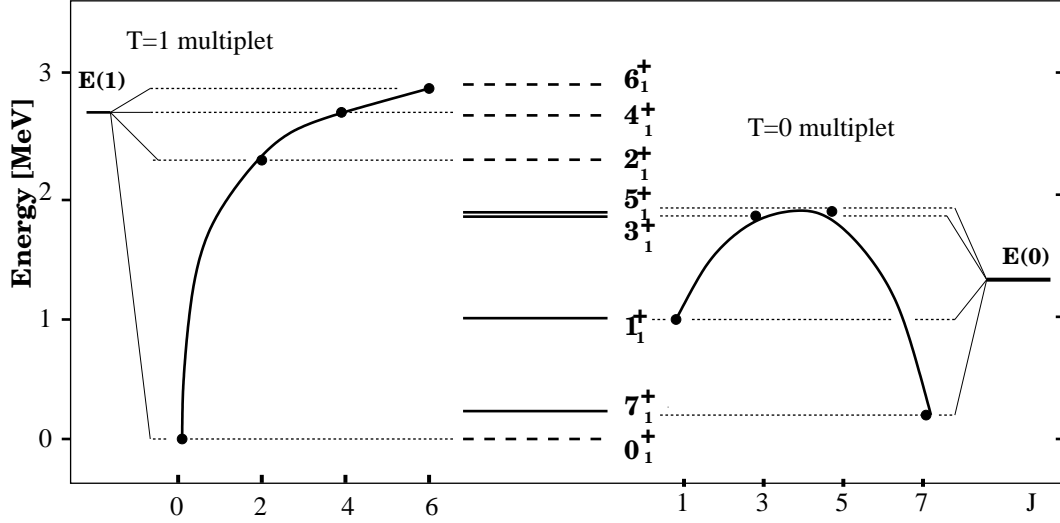


Figure 2.4: Calculated energies of  $T = 1$  and  $T = 0$  states for  $^{54}\text{Co}$  as a function of angular momentum. The excitation energy centroids  $E'(T) = E(T) - E_b(0_1^+)$  of  $T = 1$  and  $T = 0$  multiplets are shown.

energy, which is a centroid energy of multiplet states:

$$E(T) = \frac{\sum_J (2J + 1) E_T(J, j^2)}{\sum_J (2J + 1)}, \quad (2.21)$$

where  $J$  is summed over all possible values for the two-particle states  $|j^2; JT\rangle$ . It is easy to show (see [Bru77]), that for the SDI with an additional monopole part one has:

$$E(1) = -\frac{1}{4} A_{T=1} + B \quad (2.22)$$

for the centroid of  $T = 1$  multiplet and

$$E(0) = -\frac{3}{4} A_{T=0} - 3B \quad (2.23)$$

for the energy centroid of the  $T = 0$  multiplet. Thus for the used values of the SDI parameters and the modified matrix element for the  $7^+$  state one gets:

$$E_{f_{7/2}^2}(1) = -0.08 \text{ MeV} \quad \text{and} \quad E_{f_{7/2}^2}(0) = -1.52 \text{ MeV}.$$

These energy centroids and the splitting of the  $T = 1$  and  $T = 0$  states caused by the SDI are shown in Fig. (2.4). *The result above shows that the monopole part*

of the  $T = 0$  interaction is notably stronger than the monopole part of the  $T = 1$  two-body interaction. From the deviation of the energies of  $T = 1$  states from the  $T = 1$  centroid, one can see, that the  $T = 1$  pn-interaction is strongest in the  $J^\pi = 0^+$  state. This effect is related to the strong pn  $T = 1$  pairing interaction in the  $J^\pi = 0^+$  state, which is similar to the  $T = 1$  pairing for identical nucleons and corresponds to the maximal overlap of single particle orbits in the semiclassical picture. All other  $T = 1$  states are lying close to the centroid indicating a substantially weaker interaction in these states. For the  $T = 0$  multiplet one has a qualitatively different picture – the splitting is comparable for all states and there are two levels ( $J^\pi = 1^+$  and  $J^\pi = 7^+$ ) lowered in the energy. In the case of  $J^\pi = 7^+$ , maximum alignment of the single particle angular momentum of two nucleons (allowed by the Pauli principle in the case of two non-identical particles) occurs. It corresponds to the maximum overlap of the single particle orbits as in the case of the  $J^\pi = 0^+$  state, but with parallel orientation of the individual angular momenta. Thus, the interaction in this state is stronger than in other  $T = 0$  states. This explains, why the  $J^\pi = 7^+$  state is the lowest  $T = 0$  state. It is interesting to note, that the splitting between the  $J^\pi = 7^+$  and the  $J^\pi = 0^+$  states is small (0.2 MeV). This can probably be considered as an indication for strong  $T = 0$  pairing in the  $J^\pi = 7^+$  state. However, taking into account the difference in the centroid energies of  $T = 0$  and  $T = 1$  multiplets, one finds that the  $T = 0$  pairing in the  $J^\pi = 7^+$  state is approximately half as strong as the  $T = 1$  pairing in the  $J^\pi = 0^+$  state. But the interpretation of the  $T = 0$  pairing is not as transparent as the one for the  $T = 1$  pairing, and it is currently under discussion [Naz99].

### 2.6.2 M1 transitions as fine testing tools of nuclear structure

Furthermore one can note from Eqs. (2.19) and (2.20), that the energies of the two-nucleon states depend on the single particle angular momentum quantum number  $j$ . Thus one should expect qualitatively the same spectra for the one-proton-one-neutron configurations for different orbitals with the same  $j$ -value. For example, the spectra for two-nucleon configurations in  $d_{5/2}$  and  $f_{5/2}$  orbitals ( $j = 5/2$ ) should be very similar. The only difference is the global energy scale due to the mass dependence of the interaction parameters  $A_T$ . But as it is shown in the previous section, the B(M1) values for these two cases are drastically different (for the  $d_{5/2}$  orbital one has  $j = l + 1/2$  and for the  $f_{5/2}$  orbital  $j = l - 1/2$ ).

*Thus, one can conclude, that the M1 transitions are much more sensitive tools to test nuclear structure and wave functions than the excitation energies or even*

the E2 transitions, which in most cases exhibit an insensitivity to the orientation of the single particle spin with respect to the orbital angular momentum.

To show how efficient nondiagonal M1 matrix elements in the case of the  $^{54}\text{Co}$  are, our attention was focused on the M1 and E2 transition probabilities between low-lying states. From the new experimental data some very important branching ratios and multipole mixing ratios  $\delta$  are known [ScC99]. To calculate B(M1) values Eq. (2.8) was used with a quenching factor  $\alpha_q = 0.7$ . The effective proton  $e_p$  and neutron  $e_n$  charges for the E2 transition operator were chosen to get the best agreement with experimental branching ratios for both calculations. Having experimental branching ratios and multipole mixing ratios, one can get B(M1) values if lifetimes of the states or B(E2) values are known. Unfortunately, it is still very difficult to measure the lifetimes of low-lying states in  $^{54}\text{Co}$ .

However, basing on the isospin symmetry one can show, for example, that the B(E2;  $2_1^+ \rightarrow 0_1^+$ ) value in  $^{54}\text{Co}$  is comparable with the B(E2;  $2_1^+ \rightarrow 0_1^+$ ) value in  $^{54}\text{Fe}$ , which belongs to the same  $T = 1$  isobaric triplet as  $^{54}\text{Co}$ .  $^{54}\text{Co}$  has one proton more and one neutron less than  $^{54}\text{Fe}$ . Taking into account that the effective proton charge is larger than the effective neutron charge one should expect, that in  $^{54}\text{Co}$  the B(E2;  $2_1^+ \rightarrow 0_1^+$ ) value is at least not smaller than in  $^{54}\text{Fe}$ . There are many examples in lighter nuclei, even in the  $pf$ -shell, indicating that this is really true. Thus assuming that B(E2;  $2_1^+ \rightarrow 0_1^+$ ) values are equal in  $^{54}\text{Fe}$  and  $^{54}\text{Co}$ , one can get a rather realistic estimation of the B(M1;  $2_1^+ \rightarrow 1_1^+$ ) value in  $^{54}\text{Co}$ . Following this prescription, the B(M1) values were estimated in [ScC99] for some transitions which are compared to the calculated values in Table 2.2.

One sees from this comparison, that there are very strong M1 transitions in  $^{54}\text{Co}$  which are main indicators for the dominance of quasideuteron  $[\pi f_{7/2}^{-1} \times \nu f_{7/2}^{-1}]_{J,T}$  configurations. It is important to note, that aside from the strong  $1_1^+ \rightarrow 0_1^+$  transition the strong  $2_1^+ \rightarrow 1_1^+$ ,  $3_1^+ \rightarrow 2_1^+$ ,  $4_1^+ \rightarrow 3_1^+$  and  $4_1^+ \rightarrow 5_1^+$  transitions are expected in  $^{54}\text{Co}$ , too. Furthermore, it is very important to note, that this result is very different from the case of  $^{42}\text{Sc}$ . The low-lying states in  $^{42}\text{Sc}$  are usually considered as one of the best examples of the pure proton-neutron  $[\pi f_{7/2}^1 \times \nu f_{7/2}^1]_{J,T}$  configurations (see [Hey94, Tal93]), and the energies of the low-lying states are used to extract the proton-neutron two-body matrix elements of semi-empirical residual interactions for the  $f_{7/2}$  orbital. However in  $^{42}\text{Sc}$  only one strong transition is observed (see Table 2.2).

Thus, M1 transition strengths in  $^{42}\text{Sc}$  disprove the dominance of  $[\pi f_{7/2}^1 \times \nu f_{7/2}^1]_{J,T}$  configurations for most of the low-lying states in  $^{42}\text{Sc}$ , despite the fact that the behavior of the energies for the yrast states appears to be similar to the

Table 2.2: Calculated electromagnetic transition strengths for  $^{54}\text{Co}$  (column 2 and 4), experimental  $B(E2)$  values for  $^{54}\text{Fe}$  (column 3) used for the estimation of  $B(M1)$  values in  $^{54}\text{Co}$  (5th column), and experimental  $B(M1)$  values for  $^{42}\text{Sc}$  (last column). The results of calculations in the  $f_{7/2}$  configurational space are shown for the effective spin  $g$  factors  $g_s^{\text{eff}} = 0.7 \cdot g_s^{\text{free}}$  and effective charges  $e_p = 2.79$ ,  $e_n = 2.00$ .

| $(J_i, T_i) \rightarrow (J_f, T_f)$ | $B(E2; J_i \rightarrow J_f), (e^2\text{fm}^4)$ |                  | $B(M1; J_i \rightarrow J_f), (\mu_N^2)$ |                  |                  |
|-------------------------------------|--|------------------|---|------------------|------------------|
|                                     | Th.  | Expt.            | Th.                                     | Expt.            |                  |
|                                     | $^{54}\text{Co}$                               | $^{54}\text{Fe}$ | $^{54}\text{Co}$                        | $^{54}\text{Co}$ | $^{42}\text{Sc}$ |
| $(0_1^+, 1) \rightarrow (1_1^+, 0)$ | 0  |                  | 12.15                                   | $\sim 10$        | 11(4)            |
| $(2_1^+, 1) \rightarrow (1_1^+, 0)$ | 1.0  |                  | 4.63                                    | 4.2(1)           | 0.6(2)           |
| $(2_1^+, 1) \rightarrow (0_1^+, 1)$ | 126  | 129(1)           |   |                  |                  |
| $(3_1^+, 0) \rightarrow (2_1^+, 1)$ | 2.6  |                  | 4.55                                    | 4.1(5)           | -                |
| $(3_1^+, 0) \rightarrow (1_1^+, 0)$ | 141  |                  | 0                                       |                  |                  |
| $(4_1^+, 1) \rightarrow (3_1^+, 0)$ | 4.3  |                  | 4.12                                    | $> 0.9$          | 0.16(7)          |
| $(4_1^+, 1) \rightarrow (2_1^+, 1)$ | 125  | 76(16)           | 0                                       |                  |                  |
| $(4_1^+, 1) \rightarrow (5_1^+, 0)$ | 7.3  |                  | 4.28                                    | $> 0.5$          | 0.3(1)           |

one for the  $[\pi f_{7/2}^1 \times \nu f_{7/2}^1]_{J,T}$  multiplet.

*This means, that M1 transition strengths show how clean the  $[\pi f_{7/2}^1 \times \pi f_{7/2}^1]_{J,T}$  states are, and therefore are very useful tools for the determination of properties of the two-body proton-neutron residual interaction in nuclear states with well defined single particle quantum numbers.*

Based on the analysis of the new experimental data and simple theoretical results for  $^{54}\text{Co}$  presented above, *it can be concluded, that the knowledge of the structure of this nucleus is of great importance – it will help to determine the proton-neutron two body matrix elements for the  $f_{7/2}$  orbital more precisely, which in turn are crucial for the description and understanding of the structure of many  $pf$ -shell nuclei.*

The observation of the sequence of strong M1 transitions in  $^{54}\text{Co}$  directs to another very interesting phenomenon, known as magnetic rotation, which also has strong M1 transitions as main signature. The similarities and differences between the properties of quasideuteron configurations and magnetic rotation will be discussed in the following section.

## 2.7 Quasideuteron states and magnetic rotation

The regular sequences of M1  $\gamma$ -ray transitions have been observed in the near spherical neutron-deficient Pb and Bi isotopes [Cla93, Bal94] and in many nuclei of the  $A \sim 110$  Cd-Sn region [Gad97, Jen98]. The states in these bands generally have a rotational-like behavior with energies following the pattern of  $\Delta E(J) = E(J) - E(J_b) \sim A(J - J_b)^2$ , where  $J$  is the spin of the state and  $J_b$  the band head spin. However, the electromagnetic transition properties of the bands are extremely unusual as for the rotational-bands: the levels are linked by strong M1 transitions with weak E2 crossover transitions (typical  $B(M1)/B(E2)$  ratios  $\geq 20-40(\mu_N/eb)^2$ ). The shell model configurations of these states involve high- $j$  particles of one type of nucleons ( $h_{9/2}$  and  $i_{13/2}$  protons for the bands in the  $A \sim 200$  region and  $h_{11/2}$  neutrons for the bands in the  $A \sim 100$  region) and high- $j$  holes of the other type of nucleons ( $i_{13/2}$  neutrons and  $g_{9/2}$  protons for the structures in the Pb-Bi and Cd-Sn regions, respectively). Calculations by Frauendorf [Fra93] using a tilted axis cranking (TAC) model suggests that the total angular momentum  $\mathbf{J}$  is almost completely generated by the recoupling of the total proton and neutron spin vectors  $\mathbf{J}_\pi$  and  $\mathbf{J}_\nu$ , which are characterized by good quantum numbers  $J_\pi$  and  $J_\nu$ , respectively. At the band head of these particle-hole bands,  $\mathbf{J}_\pi$  and  $\mathbf{J}_\nu$  are perpendicular to each other. Higher angular momentum states might then be generated by aligning the two spin vectors along the direction of  $\mathbf{J}$  in a way that resembles the closing of the blades of a pair of shears, hence the name usually given to these structures: shears bands. A more phenomenological semiclassical description of the shears mechanism has recently been presented in terms of two long vectors [Mac98]. This model predicts a definitive signature characteristic of the shears mechanism, namely, that the intraband  $B(M1)$  transition rates, which are proportional to the square of the perpendicular component of the magnetic dipole vector (see Fig. 2.5), should decrease noticeably with increasing angular momentum. This follows from the simple geometry specified in Fig. 2.5 resulting in the following simple semiclassical expression for the  $B(M1)$  values [Mac98]:

$$B(M1; J \rightarrow J - 1) = \frac{3}{4\pi} \frac{1}{2} \bar{\mu}_\perp^2 = \frac{3}{4\pi} g_{\text{eff}}^2 J_\pi^2 \frac{1}{2} \sin^2 \theta_\pi \mu_N^2, \quad (2.24)$$

where  $g_{\text{eff}} = g_\pi - g_\nu$  is the effective  $g$ -factor,  $\tan \theta_\pi = J_\nu \sin \theta / (J_\pi + J_\nu \cos \theta)$  with  $\theta$  being the semiclassical shears angle between proton and neutron vectors:

$$\cos \theta = \frac{\vec{J}_\pi \cdot \vec{J}_\nu}{|\vec{J}_\pi| |\vec{J}_\nu|} = \frac{J(J+1) - J_\pi(J_\pi+1) - J_\nu(J_\nu+1)}{2\sqrt{J_\pi(J_\pi+1)J_\nu(J_\nu+1)}}. \quad (2.25)$$

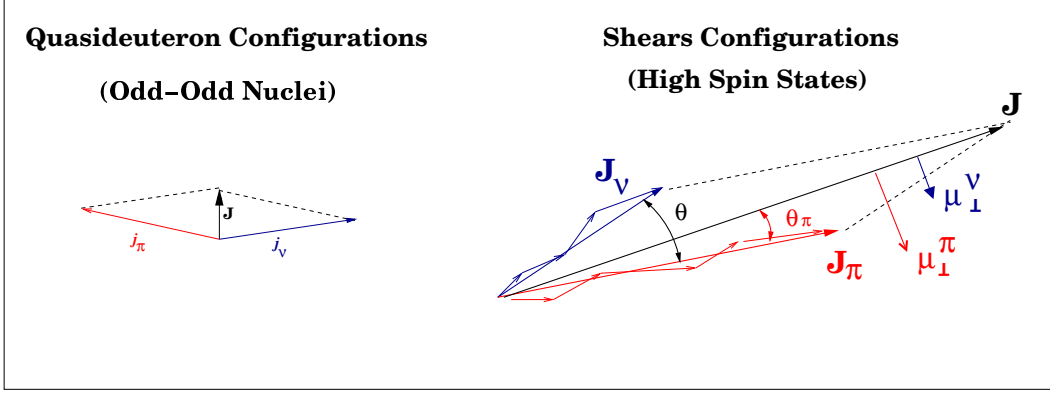


Figure 2.5: Schematic representation of quasideuteron and shears mechanism. In the case of quasideuteron configurations, angular momenta of only one proton and one neutron are involved in the generation of the total spin  $J$  near  $J \approx 0$ . In the case of shears configurations several neutrons (short vectors aligned to  $J_\nu$ ) and several proton holes (short vectors aligned to  $J_\pi$ ) are coupled to total spin  $J$  at the angle  $\theta > 90^\circ$ .

An assumption about the goodness of proton and neutron quantum numbers of angular momentum  $J_\pi$  and  $J_\nu$  in the shears model resembles very much the case of one-proton-one-neutron configurations. The only difference is, that  $J_\pi$  and  $J_\nu$  are now angular momentum quantum numbers of single particle  $j$ -orbitals and that one deals with a proton-neutron particle-particle interaction instead of a particle-hole interaction in the case of shears configurations. The latter results in a different behavior of the energies of the multiplet states, but the behavior of electromagnetic transition strengths as a function of spin  $J$  will be identical. Actually, an exact quantum mechanical expression for the  $\langle (J_\pi \times J_\nu), J' || T(M1) || (J_\pi \times J_\nu), J \rangle$  matrix elements with  $J' = J - 1$  can easily be derived:

$$\langle J' || T(M1) || J \rangle = D(J_\nu, J_\pi, J) \left[ \frac{\langle J_\nu || T_\nu(M1) || J_\nu \rangle}{f(J_\nu)} - \frac{\langle J_\pi || T_\pi(M1) || J_\pi \rangle}{f(J_\pi)} \right], \quad (2.26)$$

where  $f(J_\rho) = \sqrt{J_\rho(J_\rho + 1)(2J_\rho + 1)}$  for  $\rho = \pi, \nu$  and the only geometrical  $D(J_\nu, J_\pi, J)$  factor contains the information on the total spin  $J$ :

$$D(J_\nu, J_\pi, J) = \sqrt{\frac{[(J_{\max} + 1)^2 - J^2][J^2 - J_{\min}^2]}{4J}}, \quad (2.27)$$

where  $J_{\max} = J_\nu + J_\pi$  and  $J_{\min} = |J_\nu - J_\pi|$ .

Using the relation between the diagonal matrix elements of the  $M1$  transition operator  $T_\rho(M1)$  and the magnetic moment  $\mu_\rho$

$$\langle J || T(M1) || J \rangle = \sqrt{\frac{3}{4\pi}} \sqrt{\frac{(J_\rho + 1)(2J_\rho + 1)}{J}} \mu_\rho(J_\rho), \quad (2.28)$$

where

$$\mu_\rho(J) = \left\langle JM_J = J \left| \sum_{k=1}^{N(\rho)} g_\rho^l \cdot l_z(k) + g_\rho^s \cdot s_z(k) \right| JM_J = J \right\rangle, \quad (2.29)$$

one can show, that

$$B(M1; J \rightarrow J - 1) = \frac{3}{4\pi} \frac{D^2(J_\pi, J_\nu, J)}{2J + 1} \left[ g_\pi(J_\pi) - g_\nu(J_\nu) \right]^2 \mu_N^2, \quad (2.30)$$

where  $g_\rho(J_\rho)$  is the  $g$ -factor ( $\mu_\rho = J_\rho \cdot g_\rho(J_\rho)$ ) for the substate with spin  $J_\rho$ . By replacing  $J_\pi$  and  $J_\nu$  in Eq. (2.30) with the single particle angular momentum  $j$ , it is easy to check that Eq. (2.30) transforms to Eq. (2.8) for the quasideuteron configurations.

It is interesting to compare the exact quantum mechanical expression for  $B(M1)$  values derived above (Eq. (2.30)) with the semiclassical one given by Eq. (2.24). Assuming that  $g_{\text{eff}}$  in Eq. (2.24) and  $g_\pi(J_\pi) - g_\nu(J_\nu)$  in Eq. (2.30) are the same quantities (i.e.,  $g_{\text{eff}} = g_\pi(J_\pi) - g_\nu(J_\nu)$ ) one can show, that at the limit of very large  $J_\pi, J_\nu$  and  $J$  values (regime of shears mechanism) the geometrical factor determining the dependence of  $B(M1)$  values on total spin  $J$  approaches the semiclassical one, as it should be:

$$\frac{D^2(J_\pi, J_\nu, J)}{2J + 1} \rightarrow 2 \left( \frac{\vec{\mu}_\perp}{g_{\text{eff}}} \right)^2 = 2J_\pi^2 \sin^2 \theta_\pi. \quad (2.31)$$

However for realistic values of  $J_\pi, J_\nu$  and  $J$  there are some differences. In Fig. 2.6  $B(M1)$  values are plotted as a function of spin  $J$  using Eqs.(2.24) and (2.30) for  $J_\pi = J_\nu = 12$  (panel (a)) and  $J_\pi = J_\nu = 7/2$  (panel (b)) taking  $g_{\text{eff}} = 1.0$ . The spin value  $J_\perp$  corresponding to perpendicular coupling of proton and neutron vectors is obtained from Eq. (2.25) (putting  $\cos \theta = 0$ ) and plotted as a vertical line. As one can see from Fig. (2.6a), the behavior of both curves at  $J > J_\perp$  is almost identical. Thus, the semiclassical picture gives a perfect approximation for the  $B(M1)$  values at large spins  $J$ , where the sequences of strong but rapidly



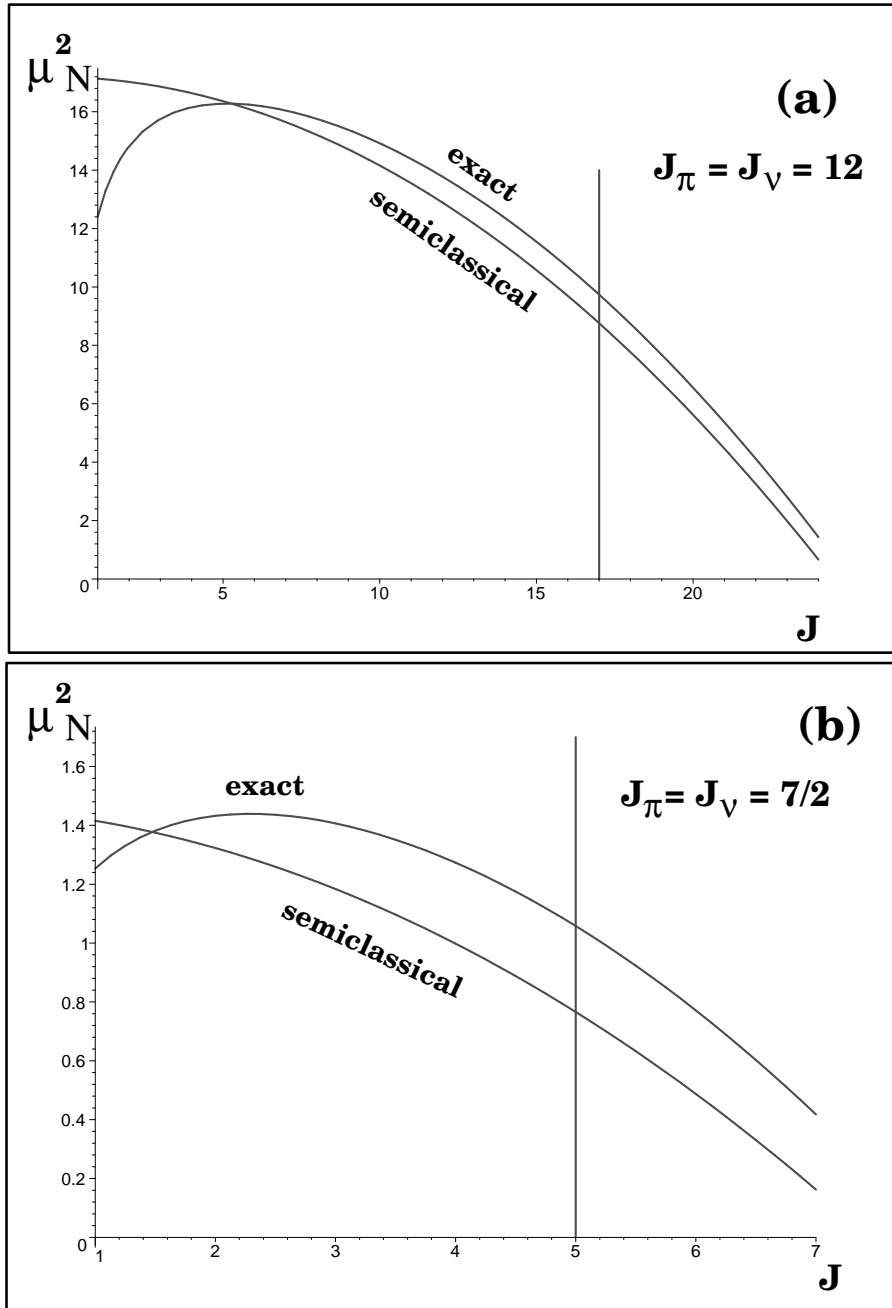


Figure 2.6:  $B(M1; J \rightarrow J - 1)$  values as a function of spin  $J$  for different spin values of proton and neutron subsystems. The curve marked with “semiclassical” corresponds to the results of the calculation using Eq. (2.24). The “exact” curves correspond to the results of Eq. (2.30). The values of the total spin corresponding to the perpendicular coupling of proton and neutron vectors are shown by a vertical line.

decreasing M1 transitions are actually experimentally observed. As one can see from Fig. (2.6), the states connected by even stronger M1 transitions are expected on the other side of the curve, i.e. for  $J < J_{\perp}$  ( $\theta < 90^{\circ}$ ). However there are only few experimental examples where shears states with  $J < J_{\perp}$  were observed for the same particle-hole structures as for long bands with  $J > J_{\perp}$ . Thus, unfavorable conditions for a shears-like mode at  $\theta < 90^{\circ}$  for particle-hole configurations are indicated.

On the contrary, for particle-particle (or hole-hole) cases there are more favorable conditions for observing shears-like states at  $180^{\circ} \geq \theta \geq 90^{\circ}$ . This is evident from the case of quasideuteron states observed in  $^{54}\text{Co}$  and discussed in the previous section. However, in this case one has short blades (completely open mini-shears) with the angle  $\theta$  inbetween, changing from  $180^{\circ}$  up to  $\approx 90^{\circ}$ . As one can see from Fig. (2.6a), in the case of short vectors one should expect only a few transitions at  $\theta > 90^{\circ}$ . Moreover, because of the large spacing between the states in this region (for example, between the  $6_1^+$  and  $7_1^+$  states in  $^{54}\text{Co}$  it is  $\approx 3$  MeV) it would be very difficult to identify transitions between them.

Another interesting point is that, despite short vectors, one has M1 transitions comparable in strength with the ones for long vectors. For example, in  $^{196}\text{Pb}$  one has  $B(\text{M1}; 28^- \rightarrow 27^-) = 4.5(10) \mu_N^2$ ,  $B(\text{M1}; 27^- \rightarrow 26^-) = 5.3(11) \mu_N^2$  [Cla98], while in  $^{54}\text{Co}$  one expects  $B(\text{M1}; 2^+ \rightarrow 1^+) = 4.2(1) \mu_N^2$ . This means, that the difference of proton and neutron  $g$ -factors ( $g_{\text{eff}}$  in Eq. (2.24)) is considerably larger in the case of short vectors. This is related to the properties of the single particle orbitals involved in these structures. Thus, in the case of quasideuteron configurations one has only an  $f_{7/2}$  orbital with  $j = l + 1/2$  for which the positive interference of spin and orbital parts of  $g_j$ -factors ( see Eq. (2.9)) results in a large value for  $g_{\text{eff}}$ . In the case of long shears vectors, for example created by two protons and two neutrons, one has the following expression for the effective  $g$ -factor:

$$g_{\text{eff}} = \frac{1}{2} \left( g_{j_1}^p + g_{j_2}^p - g_{j_3}^n + g_{j_4}^n \right), \quad (2.32)$$

where  $g_j^p$  are the Schmidt  $g$ -factors:

$$g_j^p = \frac{g_l^p l + 1/2 g_s^p}{j} \quad \text{for } j = l + 1/2 \quad (2.33)$$

$$\text{and } g_j^p = \frac{g_l^p (l + 1) - 1/2 g_s^p}{j + 1} \quad \text{for } j = l - 1/2, \quad (2.34)$$

i.e.  $g_{\text{eff}}$  is the difference of average values of  $g$ -factors for protons and neutrons. In the case of shears bands observed in the lead isotopes, the structures are thought to be built on high- $j$  proton excitations involving the  $i_{13/2}$  ( $j = l + 1/2$ ) and  $h_{9/2}$  ( $j = l - 1/2$ ) orbitals combined with  $i_{13/2}$  neutron holes. The proton  $h_{9/2}$  orbital acts destructively on the proton  $g$ -factor due to the antiparallel orientation of the single particle spin and orbital angular momentum (see Eq. (2.34)) and thus reduces the value of  $g_{\text{eff}}$ . It is a generic feature of shears structures that both  $j = l - 1/2$  and  $j = l + 1/2$  orbitals are equally represented, and thus, it explains the reduction of  $g_{\text{eff}}$ -factors for shears bands in comparison to mini-shears quasideuteron states.

From the comparison above one can draw the following conclusions:

- *The quasideuteron configurations represent the realization of a mini-shears mode (short blades) for particle-particle (hole-hole) configurations at  $180^\circ \geq \theta \geq 90^\circ$ , i.e. in the region where one has unfavorable conditions to observe shears bands built on very long blades of particle-hole configurations;*
- *There is a qualitative difference in the behavior of  $B(M1)$  values as a function of spin  $J$  for semiclassical and quantum mechanical cases for small values of spin  $J$  ( $\theta \sim 180^\circ$ ). Thus the semiclassical picture of the shears mechanism is appropriate only for  $\theta \ll 180^\circ$ ;*
- *The favorable condition for the observation of very strong  $M1$  transitions within a shears band is not just the presence of high- $j$  orbitals but the orbitals with  $j = l + 1/2$ .*

## 2.8 Intensity Relations

Similarly to the case of  $M1$  transitions discussed in the previous section, one can derive expressions for the matrix elements of the  $E2$  transition operator  $\mathbf{T}(E2) = \mathbf{T}_\pi(E2) + \mathbf{T}_\nu(E2)$ :

$$\langle J || T(E2) || J - 2 \rangle = \frac{\sqrt{6}D(J_\nu, J_\pi, J)D(J_\nu, J_\pi, J - 1)}{\sqrt{2J - 1}} \left[ q_\pi(J_\pi) + q_\nu(J_\nu) \right], \quad (2.35)$$

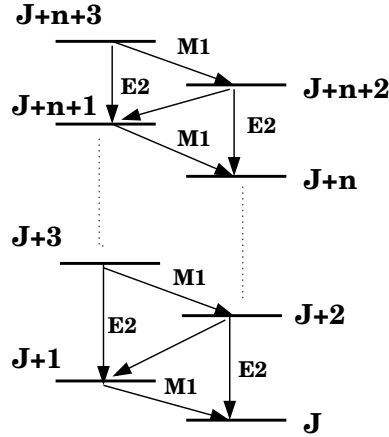


Figure 2.7: The fragment of the cascades of E2 and M1 transitions for which Eqs. (2.37), (2.38) and (2.39) are valid.

where

$$q_\rho(J_\rho) = \frac{\langle J_\rho || T_\rho(E2) || J_\rho \rangle}{\sqrt{J_\rho(J_\rho + 1)(2J_\rho + 1)(2J_\rho + 3)(2J_\rho - 1)}} = \sqrt{\frac{5}{16\pi}} \frac{Q_\rho(J_\rho)}{J_\rho(2J_\rho - 1)},$$

where  $Q_\rho$  is the static quadrupole moment of the proton ( $\rho = \pi$ ) or neutron ( $\rho = \nu$ ) subsystem in the state with spin  $J_\rho$ :

$$Q_\rho = e_\rho \sum_i \langle J_\rho M = J_\rho | 3z_i^2 - r_i^2 | J_\rho M = J_\rho \rangle, \quad (2.36)$$

with  $e_\rho$  as effective charge. The geometrical factor  $D(J_\nu, J_\pi, J)$  is defined by Eq. (2.27). Combining Eqs. (2.35) and (2.30) one finds the following interesting relation between M1 and E2 strengths for the cascades of transitions shown in Fig. 2.7

$$B(M1; J + 1 \rightarrow J) \frac{B(M1; J + 2 \rightarrow J + 1)}{B(E2; J + 2 \rightarrow J)} = \frac{[g_\pi(J_\pi) - g_\nu(J_\nu)]^4}{6 [q_\pi(J_\pi) + q_\nu(J_\nu)]^2}, \quad (2.37)$$

i.e. it is independent of the spin values of the states involved. The relation (2.37) means that, if the B-values are known for some  $J$  then there is an invariant ex-

Table 2.3: *Experimental  $B(E2)$  and  $B(M1)$  values for the shears states identified in  $^{198}\text{Pb}$ ,  $^{108}\text{Sn}$ , and  $^{139}\text{Sm}$ . In the last column the invariant quantity for a shears band defined in Eq. (2.37), deduced from the experimental data is shown for each band.*

| $^{198}\text{Pb}$ nucleus [Cla97]   |   |   |   |
|-------------------------------------|---|---|---|
| $J_i$                               | $B(M1; J_i \rightarrow J_i - 1)$<br>( $\mu_N^2$ ) | $B(E2; J_i \rightarrow J_i - 1)$<br>( $e^2\text{b}^2$ ) | Eq. (2.37)<br>( $\mu_N^4/e^2\text{b}^4$ ) |
| $J + 1$                             | $5.82^{+1.95}_{-2.59}$                            | $0.487^{+0.218}_{-0.261}$                               |   |
| $J + 2$                             | $3.17^{+0.64}_{-0.64}$                            | $0.094^{+0.037}_{-0.037}$                               | $226^{+104}_{-123}$                       |
| $J + 3$                             | $3.06^{+0.64}_{-0.97}$                            | $0.173^{+0.044}_{-0.060}$                               | $63^{+15}_{-15}$                          |
| $J + 4$                             | $2.31^{+0.63}_{-0.84}$                            | $0.107^{+0.033}_{-0.042}$                               | $73^{+18}_{-25}$                          |
| $J + 5$                             | $2.33^{+0.62}_{-0.74}$                            | $0.081^{+0.025}_{-0.028}$                               | $72^{+22}_{-28}$                          |
| $^{108}\text{Sn}$ nucleus , [Jen99] |   |   |   |
| $15^-$                              | $1.05^{+0.1}_{-0.1}$                              | $0.035^{+0.004}_{-0.005}$                               |   |
| $16^-$                              | $1.63^{+0.11}_{-0.11}$                            | $0.070^{+0.012}_{-0.010}$                               | $24^{+4}_{-4}$                            |
| $17^-$                              | $1.16^{+0.07}_{-0.16}$                            | $0.045^{+0.006}_{-0.008}$                               | $43^{+5}_{-5}$                            |
| $18^-$                              | $0.64^{+0.10}_{-0.09}$                            | $0.033^{+0.007}_{-0.006}$                               | $23^{+4}_{-4}$                            |
| $19^-$                              | $0.48^{+0.11}_{-0.11}$                            | $0.021^{+0.006}_{-0.005}$                               | $15^{+3}_{-3}$                            |
| $^{139}\text{Sm}$ nucleus [Bra96]   |   |   |   |
| $31/2$                              | $1.8^{+0.6}_{-0.6}$                               | $0.39^{+0.13}_{-0.13}$                                  |   |
| $33/2$                              | $1.5^{+0.5}_{-0.5}$                               | $0.23^{+0.08}_{-0.08}$                                  | $17^{+6}_{-6}$                            |
| $35/2$                              | $1.2^{+0.4}_{-0.4}$                               | $0.25^{+0.08}_{-0.08}$                                  | $11^{+4}_{-4}$                            |
| $37/2$                              |   |   | $12^{+4}_{-4}$                            |

pression for any other possible  $J' = J + n$ :

$$B(M1; J + 1 \rightarrow J) \frac{B(M1; J + 2 \rightarrow J + 1)}{B(E2; J + 2 \rightarrow J)} = \quad (2.38)$$

$$B(M1; J + n + 1 \rightarrow J + n) \frac{B(M1; J + n + 2 \rightarrow J + n + 1)}{B(E2; J + n + 2 \rightarrow J + n)}.$$

The property of this ‘‘three-level’’ relation is the independence of total spin  $J$  as well as of the spin of the proton ( $J_\pi$ ) and neutron ( $J_\nu$ ) subsystems. One does need to know these quantum numbers to check, whether chosen states belong to the band or not, i.e. whether they have the same structure. Moreover, one does need to know all the absolute B values, because of the presence of the  $B(M1; J + 2 \rightarrow J + 1)/B(E2; J + 2 \rightarrow J)$  ratio, which can directly be extracted from the

relative intensities. Putting  $n = 1$  in Eq. (2.38) one gets the following “four-level” relation:

$$\begin{aligned} B(E2; J + 3 \rightarrow J + 1)B(M1; J + 1 \rightarrow J) = \\ B(M1; J + 3 \rightarrow J + 2)B(E2; J + 2 \rightarrow J). \end{aligned} \quad (2.39)$$

This relation can be interpreted in the following way. The  $J + 3$  state can decay to the final state  $J$  in two alternative ways:  $J + 3 \rightarrow J + 2 \rightarrow J$  and  $J + 3 \rightarrow J + 1 \rightarrow J$ . The relation (2.39) connects the properties of these two channels. It shows that the “probability” of the  $J + 3 \rightarrow J$  decay for two alternative ways is the same.

Furthermore it is interesting to note, that the relation between E2 and M1 strengths for the intraband transitions in the frames of the rotational model has exactly the same property (see [Boh69]) as the one for the case discussed above. In the case of the rotational model, a relation similar to the one given by Eq. (2.37) was tested for several rotational bands, proving that the states belonging to the band have the same intrinsic structure.

*Having obtained the rule given by Eq. (2.37) one sees that it is not an unique property of the well deformed structures with the same intrinsic state, but it is, too, appropriate for any system consisting of two subsystems characterized by definite values of corresponding angular momentum.*

To illustrate the efficiency of Eq. (2.37) in the test of the shears band structures, a few experimental examples for shears bands in  $^{198}\text{Pb}$  [Cla97],  $^{108}\text{Sn}$  [Jen99] and  $^{139}\text{Sm}$  nuclei [Bra96] are presented in Table 2.3. One sees from this table, that the ratio defined by Eq. (2.37) is approximately constant for states belonging to the same band. Thus, it indicates that they have the same structure. However, the B(E2) and B(M1) values have to be measured more precisely to have better proof for the shears nature of the studied states.

# Chapter 3

## Quasideuteron states with deformed core

### 3.1 Rotor-plus-quasideuteron model

The study of the strong  $0_1^+ \rightarrow 1^+$  M1 transitions in odd-odd  $N = Z$  nuclei presented in Chapter 2 shows, that in spherical nuclei with one proton and one neutron above the inert doubly magic even-even  $N = Z$  core, e.g. in  ${}^6\text{Li}$ ,  ${}^{18}\text{F}$  and  ${}^{42}\text{Sc}$ , the total M1 transition strength from the yrast  $0_1^+, T = 1$  state to the  $1^+, T = 0$  states is concentrated in the  $0_1^+ \rightarrow 1_1^+$  transition. As shown above, this suggests, that the structure of the low-lying states in these nuclei is dominated by simple quasideuteron configurations. In other nuclei, which have three valence protons and three valence neutrons (like  ${}^{10}\text{B}$ ,  ${}^{22}\text{Na}$  and  ${}^{46}\text{V}$ ) or larger, equal number of valence protons and neutrons (like  ${}^{26}\text{Al}$ ), the  $0_1^+ \rightarrow 1_1^+$  transition strength is large, but nevertheless reduced by a factor  $\sim 2-3$  compared to the values for nuclei having just one valence proton and neutron. From experimental data for the nuclei mentioned above (especially for the light ones:  ${}^{10}\text{B}$ ,  ${}^{22}\text{Na}$ ,  ${}^{26}\text{Al}$ ) it follows, that they exhibit the properties of deformed nuclei. Thus, to analyze the M1 transitions in this kind of nuclei it is instructive to apply the unified model, where nucleons are supposed to move in an axially symmetric deformed field and occupy deformed Nilsson orbitals.

The basic assumption of the model [Asc68, Was71], which was applied to the deformed odd-odd  $N = Z$  nuclei in [LiL01], is, that one has one proton and one neutron outside a rotating axially deformed even-even core. The simplified version of this model was considered, neglecting the Coriolis interaction and the

residual interaction between the odd proton and odd neutron. Then the rotational motion of the nucleus is specified by the quantum numbers  $JMK$  and the total wave function has its form appropriate to a rotationally invariant system:

$$|JMK T\rangle = \sqrt{\frac{2J+1}{16\pi^2(1+\delta_{K,0})}} \left[ D_{MK}^J \Phi_{K,T} + (-1)^{J+K} D_{M-K}^J \Phi_{\bar{K},T} \right], \quad (3.1)$$

where  $\Phi_{K,T}$  is the wave function in the intrinsic system:

$$\Phi_{K,T} = \frac{\sqrt{2-\delta_{\Omega_1\Omega_2}}}{2} \left[ u_\pi(\Omega_1)u_\nu(\Omega_2) + (-1)^T u_\pi(\Omega_2)u_\nu(\Omega_1) \right] \cdot \zeta_{T_z=0}^T(1,2), \quad (3.2)$$

where  $K = \Omega_1 + \Omega_2$ ,  $u_\rho(\Omega_i)$  are single particle eigenfunctions of the Nilsson Hamiltonian with  $\Omega_i$  as 3-projection of the particle angular momenta,  $T$  is the isospin quantum number and  $\zeta_{T_z=0}^T(1,2)$  - the isospin wave function. In order to understand M1 transitions in deformed odd-odd  $N = Z$  nuclei, the representation of explicit coupling of angular momenta of the axial rotor, the odd proton, and the odd neutron was used [Boh69]. The reason for the use of this representation was the question, whether these M1 transitions are related to the QD- or spin-flip mechanism having non-collective nature or whether they are induced by the quadrupole deformation and are of collective nature. As a starting point one can use the particle-plus-rotor model basis states written in terms of spherical single-particle wave functions in a strong coupling approximation [Boh69, Gui98]:

$$|JMK\rangle = \sum_{R,j} \sqrt{\frac{(1+\delta_{KR,0})(2R+1)}{2J+1}} C_{RK_Rj\Omega}^{JK} \chi_j^\Omega \left[ |R\rangle \otimes |j\rangle \right]_M^J, \quad (3.3)$$

where  $\chi_j^\Omega$  are projection coefficients of single particle Nilsson  $[Nn_z\Lambda]\Omega$  orbitals on the spherical single particle  $|nlj\Omega\rangle$  basis [Irv72]:

$$|Nn_z\Lambda; \Omega\rangle = \sum_{j=\Omega}^{N+1/2} \chi_j^\Omega |nlj\Omega\rangle, \quad (3.4)$$

$C_{RK_Rj\Omega}^{JK}$  are Clebsch-Gordan coefficients,  $R$  is the core angular momentum quantum number and

$$\left[ |R\rangle \otimes |j\rangle \right]_M^J = \sum_{M_R,m} C_{RM_Rjm}^{JM} |RM_R\rangle \cdot |nljm\rangle$$



are weakly coupled rotor-plus-particle states (SU(2) coupling). The wave functions for two particle states coupled to the  $K_R = 0$ ,  $T = 0$  rotational core can easily be constructed applying Eq. (3.3). After some simple transformations one obtains:

$$|JMKT\rangle = \sum_{R, J_q} \sqrt{\frac{2(2R+1)}{2J+1}} C_{R0J_qK}^{JK} \left[ |R\rangle \otimes |J_q\rangle \right]_{MT_z=0}^{JT}, \quad (3.5)$$

where the  $|J_q\rangle$  is a one-proton-one-neutron state in the deformed field:

$$|J_q\rangle \equiv |J_q M_q K T\rangle = \sum_{j_1, j_2} \chi_{j_1}^{\Omega_1} \chi_{j_2}^{\Omega_2} C_{j_2 \Omega_2 j_2 \Omega_2}^{J_q K} \left[ |j_1\rangle \otimes |j_2\rangle \right]_{M_q T_z=0}^{J_q T}, \quad (3.6)$$

and  $\Omega_i$  is the Nilsson quantum number of the angular momentum projection on the symmetry axis for the odd proton or the odd neutron, the projection coefficients  $\chi_j^\Omega$  can be found in [Irv72]. The representation of the wave function in the form given by Eq. (3.5) is very convenient for finding the common and distinctive features between spherical quasideuteron and deformed rotor-plus-quasideuteron states. At first, one notes, that the wave function for the proton-neutron subsystem  $|J_q M_q K T\rangle$  is more complicated in the deformed field: excepting the quasideuteron components  $[|j_1\rangle \otimes |j_2\rangle]_{M_q, T_z=0}^{J_q T}$  with  $j_1 = j_2$  it contains also components with  $j_1 \neq j_2$ . For the deformed nuclei near closed shells, however, the quasideuteron components with  $j_1 = j_2 = N + 1/2$  are dominant, which is evident from the large values of  $\chi_j^\Omega$  coefficients [Irv72] which actually determine their weights. Secondly, the proton-neutron states  $|J_q M_q K T\rangle$  are coupled to the different states of the rotating core, and thus, the strengths for the M1 transition between states with the total spin  $J$  and  $J + 1$  contain the contribution both from the  $J_q = J \rightarrow J_q + 1 = J + 1$  transition (similar to the case of spherical quasideuteron configurations) and from different configurations with  $0 \leq J_q \leq 2j_{\max} - 1$ . At last, one sees, that there is no core contribution to the isovector M1 transitions since only the even spins of the axial rotor ( $R = 0, 2, 4, \dots$ ) contribute to the total wave function. Thus, it is impossible to construct dipole matrix elements between rotor states with  $R$  and  $R + 2$ . In the considered model the isovector M1 transitions should therefore have the same noncollective nature caused by the relative motion of the odd proton and the odd neutron.

## 3.2 Regularities for M1 transitions in deformed odd-odd $N=Z$ nuclei

Using explicit expressions for the wave functions (3.5) and (3.6) the analytical expressions for the  $B(M1)$  values were derived. Considering the particular case of the initial state characterized by  $K = 0$  and  $T = 1$  (even  $J$ ) one gets the following formula for the  $B(M1)$  values:

$$B(M1; J, K = 0 \rightarrow J', K' = \Omega'_1 + \Omega'_2) = \frac{3}{4\pi} \mu_N^2 \left[ C_{J01K'}^{J'K'} \right]^2 \Gamma^2(\Omega_1, \Omega'_1), \quad (3.7)$$

with the  $\Gamma$  representing the contributions of different single particle orbitals:

$$\Gamma(\Omega_1, \Omega'_1) = \sum_{j_1, j'_1} \chi_{j_1}^{\Omega_1} \chi_{j'_1}^{\Omega'_1} \frac{C_{j_1 \Omega_1 j'_1 \Omega'_1}^{1K'}}{\sqrt{3}} \mathcal{M}_{j_1 j'_1}, \quad (3.8)$$

where  $\mathcal{M}_{j j'} = \sqrt{j(j+1)(2j+1)} g_{IV}^j$  for  $j' = j$ , i.e. for quasideuteron configurations and  $\mathcal{M}_{j j'} = \sqrt{l(l+1)(2l+1)}(g_{IV}^{j'} - g_{IV}^j)/2$  for spin-orbit partner orbitals with  $j = l \pm 1/2, j' = l \mp 1/2$ . The difference of proton and neutron  $g$ -factors ( $g_{IV}^j = g_p^j - g_n^j$ ) is given by the Eqs. (2.9) and (2.10). When both odd particles occupy the same Nilsson level with  $\Omega \neq 1/2$ , it can be taken for granted that, the lowest  $1^+$  state in the odd-odd  $N = Z$  nucleus is a bandhead of a  $K = 0, T = 0$  ( $r = -1$ ) band. This means that both initial  $J$  and final  $J' = J + 1$  states are characterized by  $K' = K = 0$  quantum numbers and from Eq. (3.7) one obtains a simple expression for the  $B(M1)$  values which is analyzed in details in [LiL01]. The calculated and experimental  $B(M1; 0_1^+ \rightarrow 1_1^+)$  values for the deformed odd-odd  $N = Z$  nuclei with the  $1_1^+$  state characterized by  $K = 0$  are given in Table 3.1. This data are plotted in Figure 3.1, also giving the predictions for the cases where the  $g_{9/2}$  orbital ( $l = 4$ ) is expected to be dominant. *One can conclude from Table 3.1 and Figure 3.1 a surprisingly good agreement of the experimental data with the theoretical results. It means that in the deformed odd-odd  $N = Z$  nuclei considered the lowest  $1_1^+$  state corresponds to the  $K = 0$  component of the  $1^+$  quasideuteron state, while other  $K = 1$  components are shifted to higher energies.* This subsequently explains an observed decrease of the  $B(M1; 0_1^+ \rightarrow 1_1^+)$  values in the analyzed deformed nuclei in comparison to the ones containing just one valence proton and one valence neutron. Below some interesting properties of the  $\Delta K = 0, 0_1^+ \rightarrow 1_1^+$  transitions are briefly noted:

- Proportionality of  $B(M1, \Delta K = 0)$  values to  $\Omega^2$ ;

- Dominant contribution of quasideuteron configurations with  $j = l + 1/2$  to the  $B(M1, \Delta K = 0)$  values;
- Insensitivity to the quadrupole deformation  $\beta$  in the  $\Omega_{\max} = N + 1/2$  case;
- Proportionality of  $B(M1, \Delta K = 0)$  values to  $\sqrt{\beta}$  for the same values of  $\Omega$ ;
- Expectation of very strong M1 transitions in heavy odd-odd  $N=Z$  nuclei near  $^{100}\text{Sn}$ .

Using Eq. (3.7) one can also calculate the  $B(M1)$  values for the transitions in nuclei where  $j = l - 1/2$  orbitals play a dominant role. However, the problem

Table 3.1:  $B(M1)$  values for the transitions between the  $0_1^+$ ,  $K = 0$  state and the  $1_1^+$ ,  $K = 0$  state. The structure of the  $1_1^+$  states is shown in the third column, where  $(l_d j_d)$  indicates the dominant spherical component in Eq. (3.4). The calculated  $B(M1)$  values are given for the quenching factor  $\alpha_q = 0.9$ . Experimental  $B(M1)$  values shown in the last column are taken from [Fri99, BrM01, PiY01, ScC99, End93]. The summed  $B(M1)$  values defined by the Eq. (3.7) are shown in the last column. The contribution of quasideuteron configurations with  $j_d = l_d + 1/2$  are given in the column labeled by QD for comparison. For the nuclei marked with (\*) the Coriolis effect was taken into account, (see text for details).

| Nucleus           | $\beta_{\text{eff}}$ | Structure<br>( $l_d j_d, \Omega$ ) <sup>2</sup> | B(M1; $0_1^+ \rightarrow 1_1^+$ ), ( $\mu_N^2$ ) |         | $\sum_n B(M1)_n$ , ( $\mu_N^2$ ) |                               |
|-------------------|----------------------|---|--|---------|----------------------------------|-------------------------------|
|                   |                      |   | Theory,<br>$\alpha_q = 0.9$                      | Expt.   | QD<br>$\alpha_q = 1.0$           | Eq. (3.7)<br>$\alpha_q = 1.0$ |
| $^{10}\text{B}$   | 0.8                  | ( $p_{3/2}, 3/2$ ) <sup>2</sup>                 | 6.5  | 7.5(32) | 13.0                             | 15.8                          |
| $^{22}\text{Na}$  | 0.43                 | ( $d_{5/2}, 3/2$ ) <sup>2</sup>                 | 4.6  | 5.0(3)  | 15.0                             | 17.8                          |
| $^{26}\text{Al}$  | 0.38                 | ( $d_{5/2}, 5/2$ ) <sup>2</sup>                 | 9.3  | 8(2)    | 15.0                             | 18.4                          |
| $^{46}\text{V}$   | 0.23                 | ( $f_{7/2}, 3/2$ ) <sup>2</sup>                 | 3.2  | 5(2)    | 18.2                             | 21.5                          |
| $^{50}\text{Mn}$  | 0.25                 | ( $f_{7/2}, 5/2$ ) <sup>2</sup>                 | 7.2  | 6.7(14) | 18.2                             | 21.6                          |
| $^{54}\text{Co}$  | 0.16                 | ( $f_{7/2}, 7/2$ ) <sup>2</sup>                 | 12.5   | 12(2)   | 18.2                             | 21.8                          |
| $^{14}\text{N}^*$ | 0.31                 | ( $p_{1/2}, 1/2$ ) <sup>2</sup>                 | 0.05   | 0.05(2) |                                  |                               |
| $^{30}\text{P}^*$ | 0.28                 | ( $s_{1/2}, 1/2$ ) <sup>2</sup>                 | 2.0  | 1.3(1)  |                                  |                               |
| $^{34}\text{Cl}$  | 0.23                 | ( $d_{3/2}, 3/2$ ) <sup>2</sup>                 | 0.36   | 0.23(2) |                                  |                               |
| $^{38}\text{K}$   | 0.11                 | ( $d_{3/2}, 3/2$ ) <sup>2</sup>                 | 0.25   | 0.47(4) |                                  |                               |
| $^{66}\text{As}$  | 0.25                 | ( $p_{3/2}, 3/2$ ) <sup>2</sup>                 | 2.9  | -       |                                  |                               |
| $^{70}\text{Br}$  | 0.25                 | ( $f_{5/2}, 3/2$ ) <sup>2</sup>                 | 0.24   | -       |                                  |                               |

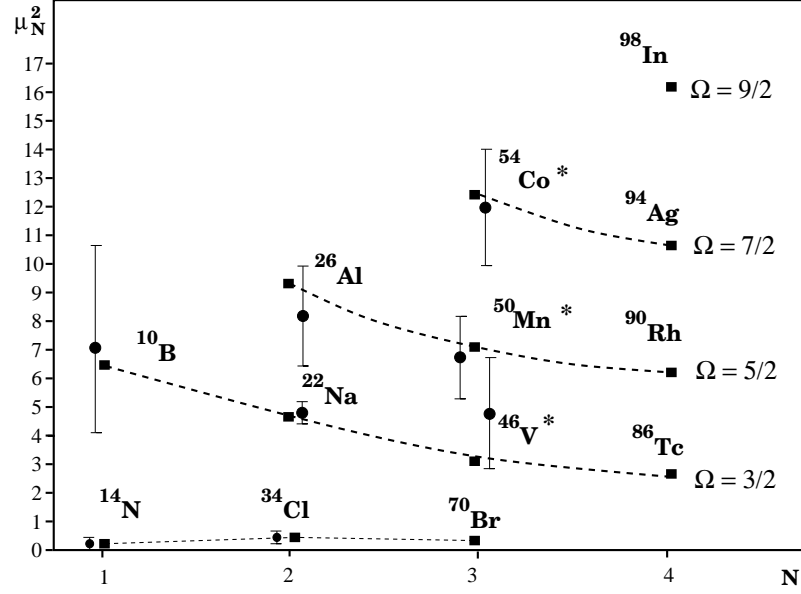


Figure 3.1: Calculated (Eq. (3.7) with  $\alpha_q = 0.9$ ) and experimental  $B(M1; 0_1^+ \rightarrow 1_1^+)$  values as a function of principal quantum number  $N$  for different values of the  $\Omega$  quantum number. The filled circles with error bars and filled squares connected with dashed lines are used for experimental and theoretical data, respectively. For the nuclei marked with an asterisk (\*), the experimental data are deduced following the procedure discussed in [LiL01]. Very small  $B(M1; 0_1^+ \rightarrow 1_1^+)$  values are shown at the bottom for some of the nuclei where the  $j = l - 1/2$  orbital is expected to be dominant.

is, that for the upper part of the harmonic oscillator shell one should deal with the Nilsson orbitals with  $\Omega = 1/2$ , and thus, one should take into account the Coriolis interaction, which mixes the  $|1^+, K = 1, (l_d, j_d, \Omega = 1/2)^2\rangle$  and the  $|1^+, K = 0, (l_d, j_d, \Omega = 1/2) \otimes (l_d, j_d, \bar{\Omega} = -1/2)\rangle$  states. Following the prescription given in [Boh69] the mixing amplitudes were estimated. For  $^{14}\text{N}$  one finds that the admixture of the  $|1^+, K = 0\rangle$  state to the  $|1^+, K = 1\rangle$  state (which is the lowest one) is  $\sim 4\%$  and for  $^{30}\text{P}$  it is  $\sim 9\%$ . Using Eq. (3.7)  $B(M1; 0_1^+, K = 0 \rightarrow 1_1^+, K_{\text{dominant}} = 1)$  values were calculated for  $^{14}\text{N}$  and  $^{30}\text{P}$  (see Table 3.1). For other nuclei of this class with  $\Omega = 3/2$ , i.e. for  $^{34}\text{Cl}$ ,  $^{38}\text{K}$ , and  $^{70}\text{Br}$ , Eq. (3.7) was directly used. The results are compared to experimental data in Table 3.1 and for some of them the data are shown in Fig. (3.1). Again a nice agreement can be seen: very small experimental  $B(M1)$  strengths are reproduced within the rotor-plus-quasideuteron model.

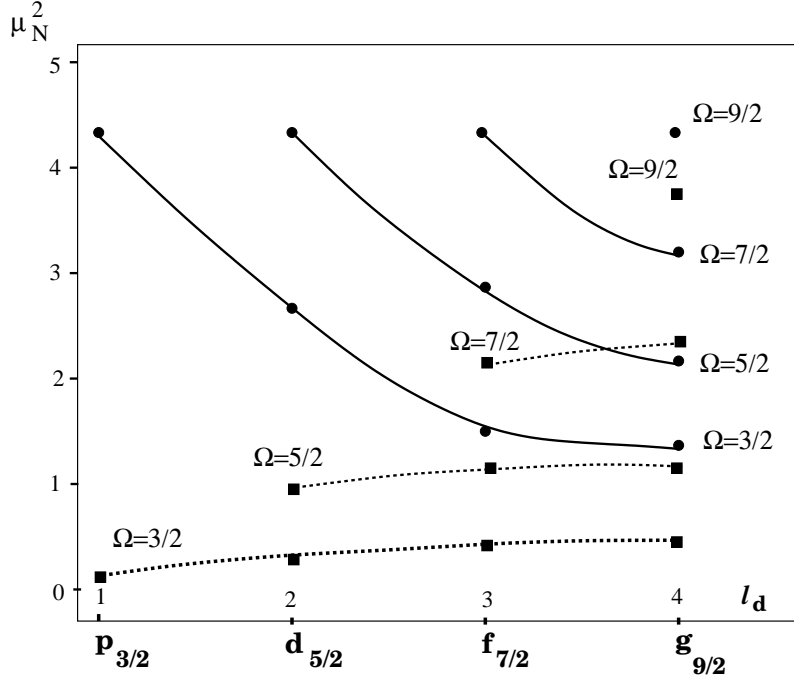


Figure 3.2: The calculated spin  $B^s(M1)$  (circles) and orbital  $B^l(M1)$  (squares) contributions to the total  $B(M1)$  strength are plotted as a function of orbital angular momentum  $l_d$  of the dominant spherical component  $j_d = l_d + 1/2$  in Eq. (3.4). The circles corresponding to the same value of  $\Omega$  are connected by solid lines and squares by dashed lines.

### 3.3 Spin and orbital contributions to M1 strengths

The analytical expression (3.7) obtained for  $B(M1)$  values makes it very simple to determine the spin and orbital contributions to the total  $B(M1)$  strength. Using Eq. (3.7) spin  $B^s(M1)$  ( $q_l = 0$ ,  $\alpha_q = 0.9$ ) and orbital  $B^l(M1)$  ( $q_l = 1$ ,  $\alpha_q = 0$ ) contributions to the total  $B(M1)$  strength were calculated. The calculated  $B^s(M1)$  and  $B^l(M1)$  values are plotted in Fig. 3.2. One notes, that in the  $\Omega = N + 1/2$  case, the spin contribution is *independent of the shell* and amounts to  $5.3 \mu_N^2$  for  $\alpha_q = 1.0$  ( $4.3 \mu_N^2$  for  $\alpha_q = 0.9$ ). The spin part of the M1 transition strength is related in a simple way with the Gamow-Teller strength for the  $0^+, T = 1, T_z = 1 \rightarrow 1^+, T = 0, T_z = 0$  transition (see [Zam88, LiG01]). Thus, the result above means, that in this specific case the GT strength amounts to 2, i.e. it is 1/3 of the Ikeda's sum rule  $3(N - Z)$  and is also independent of the shell considered. Furthermore, one notes, that the spin contribution rapidly decreases

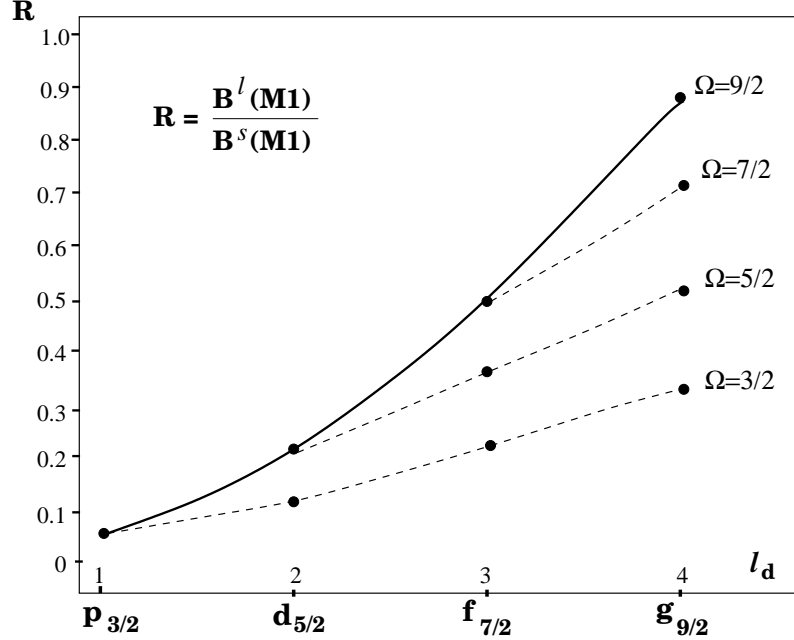


Figure 3.3: Ratio of orbital and spin contributions  $R = B^l(M1)/B^s(M1)$  as a function of the orbital angular momentum  $l_d$  of the dominant spherical component (which is shown below) for different  $\Omega$  values. The solid line corresponds to the  $\Omega_{\max} = l_d + 1/2$  case where the ratio  $R$  is the same as for the quasideuteron configurations with  $j = l_d + 1/2$ .

with increasing  $l_d$  for the same value of  $\Omega$  while the orbital part increases very slowly. For higher  $\Omega$  there is a substantial orbital contribution ( $\sim 1-2 \mu_N^2$ ) that is even comparable with the M1 strength for the collective scissors mode in heavy nuclei. However an increase of the orbital contribution with decreasing deformation can be seen, which is in contrast to the case of the scissors mode in deformed even-even nuclei.

It is also instructive to plot the ratio of the orbital and spin contributions ( $R = B^l(M1)/B^s(M1)$ ) as a function of  $l_d$  (see Fig. 3.3). The solid line connecting the ratio values for the  $\Omega_{\max} = l_d + 1/2$  cases ( $l_d = N$ , where  $N$  is a principal quantum number) represents the upper possible value of the ratio which one obtains in the case of spherical quasideuteron configurations. In this case  $R \sim l_d^2$  holds. In other cases the  $R$  value increases slower showing almost linear ( $R \sim l_d$ ) behavior. Thus the mixing of configurations caused by the quadrupole deformation tends to decrease the orbital contribution to the total  $\Delta K = 0$  M1 strength.

### 3.4 Sum Rules for M1 Strengths

As it was mentioned before, the  $K = 1$  components of quasideuteron states are expected to be shifted to higher energies. This happens if one of the two nucleons occupying a Nilsson orbital with quantum number  $\Omega$  is excited to the orbital with  $\Omega' = \Omega \pm 1$ . Then the  $B(M1; 0_1^+, K = 0 \rightarrow 1^+, K' = 1)$  values can be calculated using Eq. (3.7). This was done in [LiL01], and the calculated values were compared to the available experimental ones for some of the nuclei from  $p$ - and  $sd$ -shells. Summing up the strengths of  $0^+ \rightarrow 1^+$  transitions for the  $1^+, K = 0$  state and for one or two lowest  $1^+, K = 1$  states, one gets the value which is close to the one given by the Eq. (2.8) for the spherical quasideuteron configurations. Thus, the M1 strength for the quasideuteron  $1^+$  state is distributed over few low-lying  $K = 1$  and  $K = 0$  states. To show this, the deformed single- $j$ -orbital approximation was considered, i.e. only the dominant component is kept in Eq. (3.4). This means, that the  $\chi_j^\Omega$  coefficients with  $j \neq N + 1/2$  vanish, while  $\chi_{j=N+1/2}^\Omega = 1$ . Then using Eq. (3.7) one gets the following expressions for the  $0_{1,(T=1,K=0)}^+ \rightarrow 1_{i,(T=0,K')}^+$  transitions:

$$B(M1; 0_1^+ \rightarrow 1_{1,K=0}^+) = \frac{3}{4\pi} \Omega^2 (g_{IV}^j)^2 \mu_N^2, \quad \text{and} \quad (3.9)$$

$$B(M1; 0_1^+ \rightarrow 1_{(2,3),K=1}^+) = \frac{3}{8\pi} (j + \Omega_{2,3})(j - \Omega_{2,3} + 1) (g_{IV}^j)^2 \mu_N^2, \quad (3.10)$$

where  $\Omega_{2,3} = 1 \pm |\Omega|$ . Summing up the strengths for three  $1^+$  states one obtains

$$\sum_{i=1,2,3; K=0,1} B(M1; 0_{1,(T=1,K=0)}^+ \rightarrow 1_{i,(T=0,K)}^+) = \frac{3}{4\pi} j(j+1) (g_{IV}^j)^2 \mu_N^2, \quad (3.11)$$

which is exactly the same as the expression yielded by Eq. (2.8) for the  $0^+ \rightarrow 1^+$  transition. This exercise shows that one of the consequences of deformation is a splitting of the quasideuteron states, i.e. the splitting of the single particle states and their coupling to different spins of the deformed core result in the appearance of a few low-lying  $1^+, T = 0$  states connected with the lowest  $0^+, T = 1$  state by comparably strong M1 transitions.

As an example the results of the exact calculations using Eq. (3.7) for M1 matrix elements and calculations in the deformed single- $j$ -orbital approximation ( $f_{7/2}$  orbital) using Eqs. (3.9) and (3.10) for the three lowest  $1^+$  states are presented in Table 3.2.

Table 3.2: Individual  $B(M1; 0_1^+ \rightarrow 1_f^+, K_f)$  and summed  $\Sigma = \sum_f B(M1; 0_1^+ \rightarrow 1_f^+, K_f)$  values for the three lowest  $1^+, T = 0$  states. Results of calculations using the exact formula (3.7) and deformed single- $j$ -orbital approximation formulae (3.9) and (3.10) are shown. The bare spin  $g$ -factors were used.

| State<br>$J_f^\pi, K_f$ | $B(M1; 0_1^+ \rightarrow 1_f^+, K_f), (\mu_N^2)$ |                 |                  |                 |
|-------------------------|--|-----------------|------------------|-----------------|
|                         | $^{46}\text{V}$                                  |                 | $^{50}\text{Mn}$ |                 |
|                         | Eq. (3.7)  | Eqs. (3.9,3.10) | Eq. (3.7)        | Eqs. (3.9,3.10) |
| $1_1^+, 0$              | 3.7  | 2.6             | 8.2              | 7.2             |
| $1_2^+, 1$              | 7.6  | 8.7             | 5.6              | 6.9             |
| $1_3^+, 1$              | 5.7  | 6.9             | 3.2              | 4.1             |
| $\Sigma$                | 17.0   | 18.2            | 17.0             | 18.2            |

As one can see from Table 3.2 the contribution of the quasideuteron  $j = 7/2$  configuration is dominant for all three states, and it determines the character of the distribution of the total M1 strength among them. The summed strength for these three states in exact and approximate calculations are also very similar. However they are not exactly equal. This means that there should exist a more general sum rule. To obtain it, the  $0_1^+ \rightarrow 1_i^+$  M1 strength calculated with Eq. (3.7) were summed up for all the  $1^+, T = 0$  states constructed in the frames of a unified model for the  $N$ -shell. It was found that the sum rule determining the contribution of the odd proton and the odd neutron to the total M1 strength in the double-odd  $N=Z$  nuclei has the following form:

$$\sum_n B(M1; 0_1^+ \rightarrow 1_n^+) = \frac{3}{4\pi} \sum_{j=\Omega}^{N+1/2} \chi_j^2 \left[ j(j+1)(g_{iv}^j)^2 + \Delta_{sf}(j) \right] \mu_N^2, \quad (3.12)$$

where the first term represents the contribution of the quasideuteron configurations and the second one corresponds to the spin-flip mechanism:

$$\Delta_{sf}(j = l \pm 1/2) = \left( 1 \mp \frac{1}{2l+1} \right) \left( \frac{1}{2} - \alpha_q 4.706 \right)^2. \quad (3.13)$$

The summed strength depends only on the structure of the  $0_1^+$  state ( $\chi_j^2$ -coefficients). It is interesting to note, that the sum (3.12) can be rewritten in the following way:

$$\sum_n B(M1; 0_1^+ \rightarrow 1_n^+) = \sum_{j=\Omega}^{N+1/2} \chi_j^2 B_j^{\max}, \quad (3.14)$$



where  $B_j^{\text{max}}$  is given by Eq. (2.14) for the  $j = l + 1/2$  case and represent the M1 sum rule for the two nucleon  $|0^+, T = 1\rangle = |[j = l + 1/2]^2_{T_z=0}; J = 0\rangle$  state. For the  $|0^+, T = 1\rangle = |[j = l - 1/2]^2_{T_z=0}; J = 0\rangle$  state the spherical shell model sum rule  $B_j^{\text{max}}$  is given by

$$B_{l-\frac{1}{2}}^{\text{max}}(M1) = \frac{3}{4\pi} \left[ \frac{2l-1}{2l+1} (l+1 - \alpha_q 4.706)^2 + \frac{2l+2}{2l+1} \left( \frac{1}{2} - \alpha_q 4.706 \right)^2 \right] \mu_N^2. \quad (3.15)$$

For sum (3.15) the spin-flip contribution (second term) will be dominant, while the quasideuteron contribution (first term) is very small due to the negative interference of spin and orbital parts. However, the  $\chi_{j=l-1/2}$  amplitude in Eq. (3.14) is usually small for the lower part of any N-shell and thus the contribution to the total strength will be determined by the  $B_{j=l+1/2}^{\text{max}}$  value for which the spin-flip contribution is smaller than the quasideuteron one.

The summed B(M1) values (Eq. (3.14)) for different considered cases are shown in Table 3.1 in the last column. It is interesting to note, that for the nuclei with the same value of  $l_d, j_d$ , the summed values are very similar. Moreover, in the case of  $p$ - and  $sd$ -shells the summed M1 strengths are almost the same as the experimental B(M1;  $0_1^+ \rightarrow 1_1^+$ ) values for  $^6\text{Li}$  (15.4(4)  $\mu_N^2$ ) and  $^{18}\text{F}$  (20(4)  $\mu_N^2$ ), respectively, indicating that almost 100 % of the sum rule is exhausted by the  $1_1^+$  state in the case of one proton and one neutron above the doubly-magic core. For comparison, the B(M1) values for spherical quasideuteron configurations with a  $j = l_d + 1/2$  orbital are shown in column ‘‘QD’’. One notes, that this contribution is dominant for all cases. Furthermore, the considerable part of the summed M1 strength is distributed over the  $1_1^+$  states in deformed odd-odd  $N = Z$  nuclei. This means, that the largest part of the summed strength is concentrated in the low-lying  $1^+$  states and there is enough experimental data to support this conclusion.

### 3.5 Quasideuteron states in $^{46}\text{V}$ and $^{50}\text{Mn}$

The results of the studies presented in the previous sections were focused on the  $0_1^+ \rightarrow 1_i^+$  M1 transitions. However, the transitions between the states with spin values different from  $J = 0$  and  $J = 1$  are of great importance for a better understanding of the quasideuteron picture. Beside the yrast  $K = 0, T = 1$  and  $K = 0, T = 0$  bands the yrast  $K = 2\Omega, T = 0$  band is present at low energies in

odd-odd  $N = Z$  nuclei. In the collective model, isovector M1 transitions between the states of the  $K = 0, T = 1$  and  $K = 2\Omega, T = 0$  (with  $\Omega \geq 3/2$ ) bands are forbidden. Thus these forbidden isovector M1 transitions on the background of enhanced isovector M1 transitions can be used as effective indicators for the goodness of  $K$  as a quantum number in odd-odd  $N = Z$  nuclei. As an example, in the present subsection the results of our calculations for  $^{46}\text{V}$  and  $^{50}\text{Mn}$  are shown and compared to large scale shell model calculations performed by the Tokyo group [Fri99, ScM00] and recently available experimental data [Fri99, ScM00, PiY01, BrM01].

In order to establish the degree to which realistic shell-model calculations in the full  $pf$ -shell space generate the characteristics of collective rotational wave functions in the odd-odd  $N = Z$  nuclei,  $^{46}\text{V}$  and  $^{50}\text{Mn}$  E2 matrix elements from shell model and experiments were analyzed.

In the  $pf$ -shell model space with  $^{40}\text{Ca}$  as inert core, the low-lying states of  $^{46}\text{V}$  correspond to three protons and three neutrons which can be coupled to  $T = 0$  and  $T = 1$  states, while for  $^{50}\text{Mn}$  there are already five valence protons and five valence neutrons. Applying the Nilsson model one finds, that the symmetry properties of the intrinsic lowest states in  $^{46}\text{V}$  are firmly determined by the odd proton and odd neutron occupying the Nilsson  $[321]\Omega=3/2^-$  orbital while the other two protons and two neutrons close the  $[330]\Omega=1/2^-$  orbital. Parallel coupling ( $\Omega_\pi = \Omega_\nu = 3/2$ ) of two nucleons results in the intrinsic  $K = 3$  state. Due to the Pauli principle and signature symmetry, the states built on this intrinsic state are restricted to have isospin quantum number  $T = 0$  and negative signature  $r = -1$ . In the case of antiparallel coupling ( $\Omega_\pi = -\Omega_\nu = 3/2$ ) there are two intrinsic  $K = 0$  states with different isospin and signature symmetry:  $T = 1, r = +1$  (corresponding to the band containing even spins) and  $T = 0, r = -1$  (the band with odd spins). The consideration of  $^{50}\text{Mn}$  in the frames of the Nilsson model results in the  $K = 5$  band ( $\Omega_\pi = \Omega_\nu = 5/2$ ) and two  $K = 0$  bands ( $\Omega_\pi = -\Omega_\nu = 5/2$ ) similarly to the situation in  $^{46}\text{V}$ . Then, in the framework of the rotational model the E2 transition strengths within a single band can be calculated using the standard formula:

$$B(E2; J_i, K \rightarrow J_f, K) = \frac{5}{16\pi} e^2 Q_0^2 \left\langle J_i K 2 0 \left| J_f K \right. \right\rangle^2, \quad (3.16)$$

where the intrinsic quadrupole moment  $Q_0$  is related to the deformation parameter  $\beta$  by

$$Q_0 = \frac{3}{\sqrt{5\pi}} Z R_0^2 \beta \left( 1 + \frac{2}{7} \sqrt{\frac{5}{\pi}} \beta \right). \quad (3.17)$$

### 3.5.1 Identification of $K = 0, T = 1$ bands

To check, which levels can possibly correspond to the same stable intrinsic  $K$ -state,  $B(E2)$  values for the  $K = 0$  case were calculated using Eq. (3.16) choosing the value of the deformation parameter that yields the best agreement with shell model and experiment for the few transitions between the lowest  $K = 0, T = 1$  states. The results of the collective model are compared to the shell model results and new experimental data in Table (3.3).

Table 3.3: *The calculated and experimental  $B(E2)$  values for the isoscalar transitions for  $K = 0$  states in  $^{46}\text{V}$  and  $^{50}\text{Mn}$ . The results of the collective rotational model (Eq. 3.16) are given in the column R+QD. The values of the quadrupole deformation parameter  $\beta$  used for the calculations are shown for both nuclei. The results of Elliott's  $SU(3)$  model are given in column  $SU(3)$ . The shell model results for the KB3 residual interaction with standard effective charges ( $e_p=1.5, e_n=0.5$ ) are shown in the column KB3. Available experimental data is given in the column labeled with "Expt."*

| $J_i \rightarrow J_f$       | $^{46}\text{V}, \beta=0.23$       |     |       |            | $J_i \rightarrow J_f$     | $^{50}\text{Mn}, \beta=0.25$      |     |
|-----------------------------|-----------------------------------|-----|-------|------------|---------------------------|-----------------------------------|-----|
|                             | R+QD.                             | KB3 | SU(3) | Expt.      |                           | R+QD.                             | KB3 |
| K=0,T=1                     | [e <sup>2</sup> fm <sup>4</sup> ] |     |       |            | K=0,T=1                   | [e <sup>2</sup> fm <sup>4</sup> ] |     |
| $2_1^+ \rightarrow 0_1^+$   | 127                               | 143 | 127   | 137(35)    | $2_1^+ \rightarrow 0_1^+$ | 202                               | 220 |
| $4_2^+ \rightarrow 2_1^+$   | 183                               | 187 | 175   | $\geq 169$ | $4_2^+ \rightarrow 2_1^+$ | 289                               | 298 |
| $6_2^+ \rightarrow 4_2^+$   | 201                               | 175 | 177   |            | $6_2^+ \rightarrow 4_2^+$ | 318                               | 255 |
| $8_2^+ \rightarrow 6_2^+$   | 211                               | 168 | 163   |            |                           |                                   |     |
| $10_2^+ \rightarrow 8_2^+$  | 216                               | 124 | 136   |            |                           |                                   |     |
| $12_2^+ \rightarrow 10_2^+$ | 220                               | 54  | 99    |            |                           |                                   |     |
| $14_2^+ \rightarrow 12_2^+$ | 222                               | 53  | 54    |            |                           |                                   |     |
| K=0,T=0                     |                                   |     |       |            | K=0,T=0                   |                                   |     |
| $3_2^+ \rightarrow 1_1^+$   | 164                               | 189 | 161   |            | $3_1^+ \rightarrow 1_1^+$ | 260                               | 272 |
| $5_2^+ \rightarrow 3_2^+$   | 193                               | 159 | 173   |            | $5_2^+ \rightarrow 3_1^+$ | 306                               | 227 |

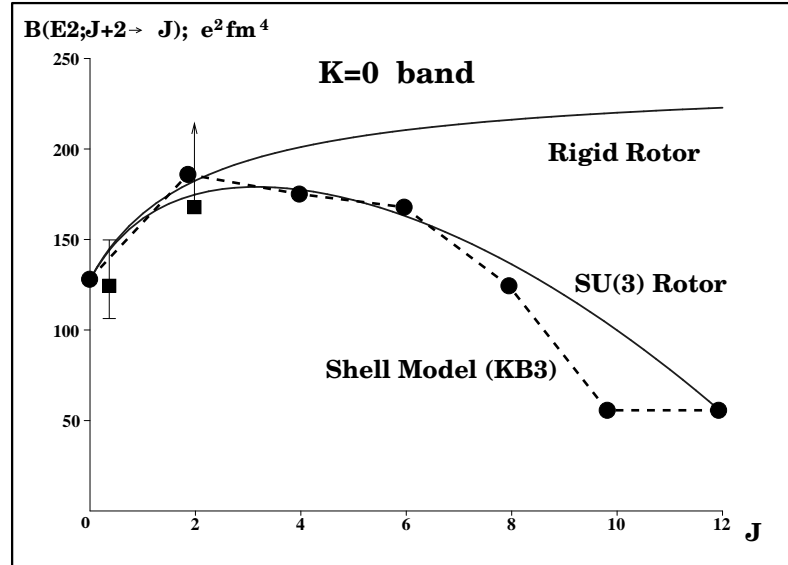


Figure 3.4: Comparison of the  $B(E2; J+2 \rightarrow J)$  values for the  $K = 0, T = 1$  band in  $^{46}\text{V}$  calculated in shell model, collective rotational model and  $SU(3)$  model. The rotational and  $SU(3)$  model results are plotted with a solid line. The shell model results are shown with circles connected by dashed lines. Experimental values are shown with squares and error bars.

One notes from Table 3.3, that the  $B(E2)$  values between  $K = 0, T = 1$  states in the collective model and the  $T = 1$  states with even spins  $J$  in the shell model are rather similar for the lowest states. However, in the shell model one observes a decrease of  $B(E2)$  values starting from  $J_i^\pi = 6_2^+$ , while in the collective model  $B(E2)$  values continue to increase. This effect finds its explanation in the microscopic character of the shell model: the valence nucleons in an appropriate configurational space can only be coupled to some certain maximum spin value  $J_{\max}$ , while in the idealized case of the collective rotational model there is no upper limit for the spin value of the band. The model, which nicely establishes the bridge between microscopic and collective rotational model, is the  $SU(3)$  model [Ell58]. It imposes a compactness condition on the sequences of the rotational states, that naturally results in the truncation of the band. In the simplest case of the axial symmetry the rotational wave functions of the ground band are characterized by the  $SU(3)$  irreducible representation  $(\lambda, 0)$ , where  $J_{\max} = \lambda$ . In this case the Elliott model yields the following expression for the  $B(E2)$  values of the

$K = 0$  band:

$$B(E2; J + 2 \rightarrow J) = \frac{5}{16\pi} e^2 Q_0^2 \langle J+2020 | J0 \rangle^2 \left[ 1 - \frac{J(J+3)}{\lambda(\lambda+3)} \right], \quad (3.18)$$

which differs from Eq. (3.16) by an additional geometrical factor that involves the quantum number  $\lambda$ . From Eq. (3.18) one can easily see, that for the  $2^+ \rightarrow 0^+$  transition the SU(3) and collective model results are identical. But at the top of the band ( $J = J_{\text{max}} = \lambda$ ) the B(E2) strength vanishes in the Elliott model, indicating band termination. Taking  $\lambda = 14$  (it is an appropriate value for 3 protons and 3 neutrons in  $N = 3$  harmonic oscillator shell [Ell58]) and using Eq. (3.18), B(E2) values for the  $T = 1, K = 0$  band in  $^{46}\text{V}$  were calculated. The results are shown in Table 3.3 in column SU(3) and plotted in Figure 3.4. One notes from Figure 3.4 an unexpectedly similar behavior of the B(E2) strengths in the full  $pf$ -shell model calculations and the SU(3) model. At the present moment only few experimental B(E2) values are known for the  $T = 1, K = 0$  band (see Table 3.3 and Figure 3.4). Thus, it would be very interesting to test the shell model predictions (which reproduce the results of the SU(3)-rotor model) for higher spins.

### 3.5.2 Identification of $K = 3, T = 0$ and $K = 5, T = 0$ bands

Furthermore based on the comparison of the collective rotational model, the shell model and experimental data, one can identify (see Table 3.4)  $T = 0$  states belonging to the  $K = 3$  band in  $^{46}\text{V}$  and the  $K = 5$  band in  $^{50}\text{Mn}$ . It is generally accepted that large  $\Delta J = 2$  E2 matrix elements are indicators of collectivity. But it must be stressed here, that this is true only for  $K = 0$  bands while for higher  $K$  bands this statement is valid only in the limit of high spins. However, the behavior of the E2 transition matrix elements between the several lowest states belonging to the band with high  $K$  (in our case  $K = 3$  for  $^{46}\text{V}$  and  $K = 5$  for  $^{50}\text{Mn}$ ) is qualitatively different from the  $K = 0$  case:  $\Delta J = 2$  transitions are a few times weaker than the  $\Delta J = 1$  ones. This is nicely illustrated in Table 3.4 and Fig. 3.5. Thus, at first glance, the small value of the  $5_1^+ \rightarrow 3_1^+$  E2 transition strength in  $^{46}\text{V}$  alone can be misunderstood as an indicator of non-collective or weakly collective states. But in a combination with the strong  $4_1^+ \rightarrow 3_1^+$  E2 transition it becomes an important fingertip to the formation of an intrinsic  $K = 3$  state. Furthermore, one notes remarkably good agreement of the shell model results with rotational model ones for higher spins, where experimental data is not available. For the  $J + 1 \rightarrow J$  E2 transitions one has perfect agreement up to  $J = 10$ , with the exception of two B(E2) values (see Fig. 3.5). The shell model results for  $J + 2 \rightarrow J$

Table 3.4: Calculated and experimental  $B(E2)$  values for allowed and forbidden isoscalar transitions in  $^{46}\text{V}$  and  $^{50}\text{Mn}$ . The results of the collective rotational model (Eq. 3.16) are given in the column R+QD. The values of the quadrupole deformation parameter  $\beta$  used for the calculations are shown for both nuclei. The shell model results for the KB3 residual interaction with standard effective charges ( $e_p=1.5, e_n=0.5$ ) are shown in column KB3. Available experimental data is given in the column labeled with "Expt."

| $J_i \rightarrow J_f$     | $^{46}\text{V}, \beta=0.23$          |     |         | $J_i \rightarrow J_f$     | $^{50}\text{Mn}, \beta=0.25$         |     |         |
|---------------------------|--------------------------------------|-----|---------|---------------------------|--------------------------------------|-----|---------|
|                           | R+QD.                                | KB3 | Expt.   |                           | R+QD.                                | KB3 | Expt.   |
| <b>K=3, T=0</b>           | <b>(<math>e^2\text{fm}^4</math>)</b> |     |         | <b>K=5, T=0</b>           | <b>(<math>e^2\text{fm}^4</math>)</b> |     |         |
| $4_1^+ \rightarrow 3_1^+$ | 223                                  | 234 | 200(50) | $6_1^+ \rightarrow 5_1^+$ | 305                                  | 293 |         |
| $5_1^+ \rightarrow 3_1^+$ | 54                                   | 65  | 66(14)  | $7_1^+ \rightarrow 5_1^+$ | 49                                   | 48  |         |
| $5_1^+ \rightarrow 4_1^+$ | 208                                  | 209 | -       | $7_1^+ \rightarrow 6_1^+$ | 361                                  | 285 |         |
| $6_1^+ \rightarrow 4_1^+$ | 96                                   | 79  | -       | $8_1^+ \rightarrow 6_1^+$ | 99                                   | 85  | >37     |
| $6_1^+ \rightarrow 5_1^+$ | 170                                  | 159 | -       | $9_1^+ \rightarrow 7_1^+$ | 142                                  | 152 | 145(22) |
| $7_1^+ \rightarrow 5_1^+$ | 126                                  | 62  | 98(20)  |                           |                                      |     |         |
| $7_1^+ \rightarrow 6_1^+$ | 136                                  | 131 | -       |                           |                                      |     |         |
| $8_1^+ \rightarrow 6_1^+$ | 147                                  | 114 | -       |                           |                                      |     |         |
| $8_1^+ \rightarrow 7_1^+$ | 110                                  | 26  | -       |                           |                                      |     |         |
| $9_1^+ \rightarrow 7_1^+$ | 163                                  | 145 | -       |                           |                                      |     |         |
|                           | $\Delta K = 3, \Delta T = 0$         |     |         |                           | $\Delta K = 5, \Delta T = 0$         |     |         |
| $3_2^+ \rightarrow 4_1^+$ | 0                                    | 7.5 | <18     | $5_2^+ \rightarrow 5_1^+$ | 0                                    | 0.2 |         |
| $5_2^+ \rightarrow 3_1^+$ | 0                                    | 7.3 |         | $3_1^+ \rightarrow 5_1^+$ | 0                                    | 0.3 |         |
| $5_2^+ \rightarrow 4_1^+$ | 0                                    | 9.9 | -       | $5_2^+ \rightarrow 6_1^+$ | 0                                    | 4.0 |         |
| $5_2^+ \rightarrow 6_1^+$ | 0                                    | 2.6 | -       | $7_2^+ \rightarrow 5_1^+$ | 0                                    | 4.3 |         |

E2 transitions deviate more from the rotational model results for higher spins, but the characteristic behavior is rather similar. The observations above are in favor of our conclusion about the  $K = 3$  band in  $^{46}\text{V}$ . However, there are indications of more complicated structures of the states in the high spin region, that

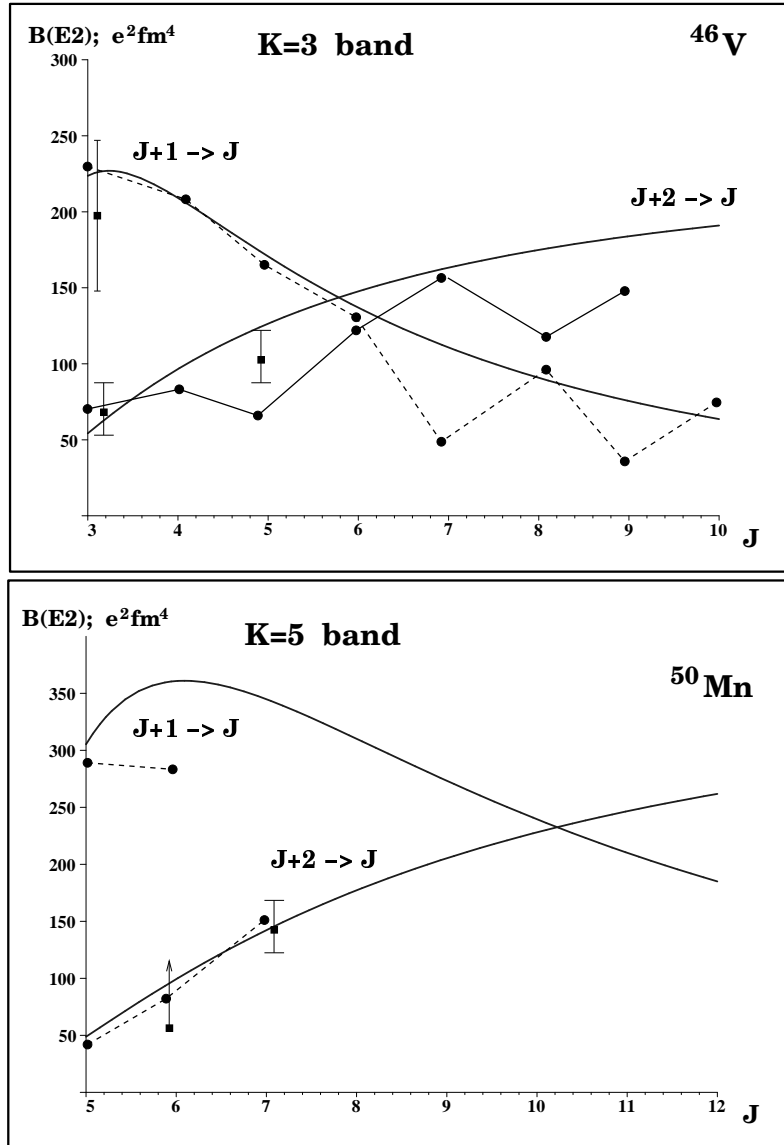


Figure 3.5: Comparison of the  $B(E2; J_i \rightarrow J_f)$  values for the  $K = 3, T = 0$  band in  $^{46}\text{V}$  and the  $K = 5, T = 0$  band in  $^{50}\text{Mn}$  calculated in the shell model and the collective rotational model. Rotational model results are plotted with a solid line. Shell model results are shown with circles connected with dashed and solid lines. Experimental data is shown with squares and error bars.

could probably be due to the interplay of collective and single-particle degrees of freedom. For  $^{50}\text{Mn}$  there is less experimental information and fewer shell model results are known. However, similar to the  $^{46}\text{V}$  case discussed above, the available data indicates the presence of the  $K = 5, T = 0$  band. The goodness of  $K$  as a quantum number can also be addressed by analyzing E2 matrix elements between the states of different bands. In frames of the rotational model, these E2 matrix elements should vanish. The shell model B(E2) values for the transitions between

Table 3.5: Calculated and experimental B(M1) values for the isovector transitions in  $^{46}\text{V}$  and  $^{50}\text{Mn}$ . The results of the collective rotor-plus-quasideuteron model (Eq. 2.8) are given in the column R+QD. The quenching factor value of  $\alpha_q = 0.9$  was used for the calculations. The shell model results for the KB3 residual interaction with bare g-factors are shown in the column KB3. Experimental data for  $^{46}\text{V}$  are given in the column labeled with "Expt".

| $J_i \rightarrow J_f$     | $^{46}\text{V}, (\mu_N^2)$   |       |             | $J_i \rightarrow J_f$     | $^{50}\text{Mn}, (\mu_N^2)$  |      |            |
|---------------------------|------------------------------|-------|-------------|---------------------------|------------------------------|------|------------|
|                           | R+QD                         | KB3   | Expt.       |                           | R+QD                         | KB3  | Expt.      |
|                           | $\Delta K = 0, \Delta T = 1$ |       |             |                           | $\Delta K = 0, \Delta T = 1$ |      |            |
| $0_1^+ \rightarrow 1_1^+$ | 3.24                         | 3.80  | $\geq 2.31$ | $0_1^+ \rightarrow 1_1^+$ | 7.23                         | 8.7  |            |
| $2_1^+ \rightarrow 1_1^+$ | 1.30                         | 0.80  | -           | $2_1^+ \rightarrow 1_1^+$ | 2.89                         | 1.94 | -          |
| $3_2^+ \rightarrow 2_1^+$ | 1.39                         | 1.25  | 1.98(71)    | $3_1^+ \rightarrow 2_1^+$ | 3.09                         | 3.73 | 2.7(6)     |
| $4_2^+ \rightarrow 3_2^+$ | 1.44                         | 0.85  | $\geq 0.52$ | $4_1^+ \rightarrow 3_1^+$ | 3.21                         | 2.71 | $\geq 0.8$ |
| $5_2^+ \rightarrow 4_2^+$ | 1.47                         | 1.17  | $\geq 0.41$ | $5_2^+ \rightarrow 4_1^+$ | 3.28                         | 3.46 | -          |
| $6_2^+ \rightarrow 5_2^+$ | 1.50                         | 1.07  | -           | $6_2^+ \rightarrow 5_2^+$ | 3.33                         | 1.73 | $\geq 0.6$ |
| $7_2^+ \rightarrow 6_2^+$ | 1.51                         | 0.07  | -           | $7_2^+ \rightarrow 6_2^+$ | 3.37                         | 1.59 |            |
|                           | $\Delta K = 3, \Delta T = 1$ |       |             |                           | $\Delta K = 5, \Delta T = 1$ |      |            |
| $3_1^+ \rightarrow 2_1^+$ | 0.0                          | 0.21  | $\geq 0.01$ | $5_1^+ \rightarrow 4_1^+$ | 0.0                          | 0.04 |            |
| $4_2^+ \rightarrow 3_1^+$ | 0.0                          | 0.08  | $\geq 0.01$ | $6_2^+ \rightarrow 5_1^+$ | 0.0                          | 0.28 |            |
| $5_1^+ \rightarrow 4_2^+$ | 0.0                          | 0.02  | $\geq 0.02$ | $7_1^+ \rightarrow 6_2^+$ | 0.0                          | 1.32 |            |
| $4_2^+ \rightarrow 4_1^+$ | 0.0                          | 0.003 | $\geq 0.01$ |                           |                              |      |            |
| $7_1^+ \rightarrow 6_2^+$ | 0.0                          | 1.20  | -           |                           |                              |      |            |



some of the states from  $K = 0, T = 0$  and  $K = 3, T = 0$  ( $K = 5, T = 0$ ) bands in  $^{46}\text{V}$  ( $^{50}\text{Mn}$ ) are shown in Table 3.4. The values are not zero, but on the average they are significantly smaller (a factor of 100 for the lowest states) than the corresponding intraband transitions.

### 3.5.3 $\Delta K = 0, \Delta T = 1$ and $\Delta K = 3, \Delta T = 1$ M1 transitions

Having established the collective properties of the wave functions, one can turn to the M1 transitions. One can check, how good M1 transitions in  $^{46}\text{V}$  and  $^{50}\text{Mn}$  fit into the collective picture. Using Eq. (2.8),  $B(\text{M1})$  values for  $\Delta T = 1, \Delta K = 0$  transitions were calculated. The results of the calculations for  $^{46}\text{V}$  and  $^{50}\text{Mn}$  are

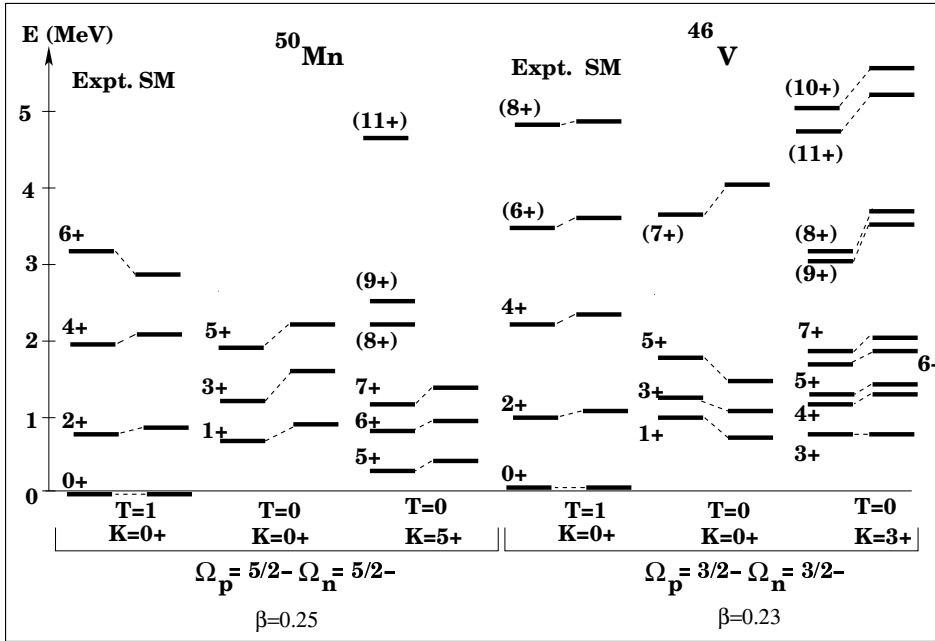


Figure 3.6: Comparison of experimental (Expt.) and Shell Model (SM) low-spin level schemes of  $^{50}\text{Mn}$  and  $^{46}\text{V}$ . The band classification of the states is based on theoretical (Shell Model and Collective Model) and experimental  $B(E2)$  values. The levels with spin values given in parenthesis were not observed in present experiments. The asymptotic Nilsson quantum number of the 3-projections of the odd proton and the odd neutron angular momentum in the intrinsic system are shown below. The main spherical component of the two nucleon configuration in a deformed field are given, too.

shown in Table 3.5.

As it can be seen from this table, the collective model reproduces both the large shell model B(M1) values and experimental B(M1) values for  $\Delta K=0$  transitions with good accuracy. Furthermore the  $\Delta T = 1$  M1 transitions calculated in the shell model between the states from supposed  $K = 0$  and  $K = 3$  ( $K = 5$ ) bands (which are forbidden in the collective model) are strongly suppressed in comparison to the  $\Delta K = 0, \Delta T = 1$  transitions. Finally, based on the analysis above, levels observed in  $^{46}\text{V}$  and  $^{50}\text{Mn}$  were grouped into bands as shown in Fig. (3.6).

The analysis of the spectra shows that the excitation energies of the states do not follow the simple  $J(J + 1) - K^2$  formula as it is for rotational bands. This deviation is especially obvious for the  $K = 3$  band, where one actually observes doublets of states with spins  $J$  and  $J + 1$ . These deviations can probably be attributed to the residual interaction of the odd proton and odd neutron and the Coriolis interaction, which had not been taken into account.

Furthermore, as seen from the shell model results for the  $J^\pi = 7_{1,2}^+$  states (see Table 3.5), the simple regularities noted for M1 transitions for other low-lying states suddenly disappear. The  $7_2^+, T = 0, K = 0 \rightarrow 6_2^+, T = 1, K = 0$  M1 transition becomes very weak while the strength of the  $7_1^+, T = 0, K = 3 \rightarrow 6_2^+, T = 1, K = 0$  M1 transition increases. This means that for the  $7_{1,2}^+, T = 0$  states from shell model,  $K$  can not be treated as a good quantum number despite the fact that B(E2) values identify the  $7_1^+, T = 0$  state as a member of the  $K = 3$  band in  $^{46}\text{V}$  (see Table 3.4). This could be related to the spin dependence of the deformation  $\beta$  or a strong band mixing.

Thus, it would be very interesting to find a simple explanation of this puzzling problem and to check experimentally what is happening in this region.

*Concluding, a rather good approximation for the realistic wave functions of the low-lying states in  $^{46}\text{V}$  and  $^{50}\text{Mn}$ , which can be characterized by the  $K$ -quantum number, was found. However, the deviations of experimental and shell model excitation energies from rotational model results, as well as the more complex behavior of electromagnetic transitions matrix elements between the states with higher spin values, mean that rotational collectivity for  $^{46}\text{V}$  and  $^{50}\text{Mn}$  is well approached for low-lying states only.*

# Chapter 4

## Summary

The study of odd-odd  $N = Z$  nuclei provides much insight into systems of many strongly interacting particles. The results of the studies presented in this work show that odd-odd  $N = Z$  nuclei are excellent sources of information on the properties of the proton-neutron force. One of the most powerful tools to obtain such information are isovector M1 transitions. The drastic difference between nondiagonal isovector M1 matrix elements for different two-nucleon configurations, emphasized in this work, makes the M1 transitions very helpful for the identification of the specific configurations. Putting forward the simple concept of quasideuteron configurations, it is shown, that the degrees of freedom related to the dynamics of the odd proton and the odd neutron determine character and intensity of the isovector M1 transitions between the states with  $T = 0$  and  $T = 1$  in odd-odd  $N = Z$  nuclei.

With the identification of a sequence of strong isovector M1 transitions in  $^{54}\text{Co}$  the dominant influence of the  $[\pi f_{7/2} \times \nu f_{7/2}]^{J,T}$  quasideuteron configurations on the structure of the low-lying states in this nucleus is demonstrated. Analyzing the low-energy spectra of  $^{54}\text{Co}$ , the important properties of the proton-neutron interaction in the states dominated by the quasideuteron configurations were established. It was found that, the monopole part of proton-neutron interaction in the  $T = 0$  channel is considerably stronger than in the  $T = 1$  channel, and that there is no unambiguous indication for strong isoscalar pairing phenomena which one has actually for isovector pairing.

The use of analytical methods in the present work helped to link the quasideuteron mode with the recently discovered phenomenon of magnetic rotation. The strong M1 transitions between the states with fixed proton as well as neutron structures is a main signature for both phenomena. The conclusion drawn from the comparison of two modes is that the quasideuteron states represent a

small scale analogue of the shears states but under conditions which are believed to be unfavorable for long shears bands. One more phenomenon, which is closely related to the latter two and which is also characterized by enhanced M1 transitions, is the scissors mode and the mixed-symmetry excitations connected with it. The recent identification of mixed-symmetry states in near-spherical nuclei  $^{94}\text{Mo}$  and  $^{96}\text{Ru}$  has motivated the study of these states within the spherical shell model. The results of our extended studies were published in a series of papers recently (see Refs. [LiN00,KIP01,BrC01,Fra01,BrH00,PiT00,BrT99] in the List of Publications following this Chapter). They are fully published and therefore are not included in the thesis. These studies have revealed the microscopic origin of the  $F$ -spin symmetry and the similarities of  $F$ -spin and isospin symmetry, proved the existence of both symmetric and mixed-symmetry quadrupole phonon excitations and shown the effects caused by the interplay between spin and orbital degrees of freedom on the properties of mixed-symmetry states in near-spherical even-even nuclei. It is very interesting to note, that for quasideuteron states, shears states, and mixed-symmetry two-phonon states, one can even use the same analytical expression (2.30) from Chapter 2 to estimate  $B(M1)$  values. The only difference is the input: spin values for proton  $J_\pi$  and neutron  $J_\nu$  subsystems and quantum numbers of single particle orbitals involved, which actually give the information on the kind of phenomenon one deals with and subsequently on the driving part of the proton-neutron forces for the corresponding phenomenon. Thus, these three phenomena provide supplementary information on the proton-neutron interaction under different conditions and in different regions of excitation energy and spin.

It is shown in the present work, that in deformed odd-odd  $N = Z$  nuclei the quadrupole deformation governs the collective dynamics of the nucleons, which is indicated by the regular behavior of strong E2 transition strengths, and causes the fragmentation of the isovector M1 strength. The studies of the latter effect shows that the quasideuteron configurations retain their individual properties in a deformed field despite the well pronounced collective effects. Studying the odd-odd  $N = Z$  nuclei  $^{46}\text{V}$  and  $^{50}\text{Mn}$ , the high- $K$ ,  $T = 0$  bands were identified at low energies in these nuclei. It was found, that the behavior of the intraband  $B(E2)$  values as a function of spin  $J$  for these bands ( $K = 3$  for  $^{46}\text{V}$  and  $K = 5$  for  $^{50}\text{Mn}$ ) is very different from the one for  $K = 0$  bands. Identifying very weak isovector  $\Delta K = 3$  and  $\Delta K = 5$  M1 transitions, it is shown, that the quasideuteron picture allows a critical assessment of collective  $K$ -quantum number selection rules for low-lying states in odd-odd  $N = Z$  nuclei, which nicely arise in full  $pf$ -shell model results, too. This was established by treating the quasideuteron degrees of freedom explicitly in the rotor-plus-particles model. Having derived

analytical expressions for isovector M1 transition strengths it was found, that only the one proton and one neutron above the rotating even-even  $N=Z$  core contribute to the isovector M1 transition strengths for the low-lying states. A very good agreement between the experimental and theoretical  $B(M1;0_1^+ \rightarrow 1_1^+)$  values in odd-odd  $N = Z$  nuclei indicated in this thesis, helps to extend the systematic for  $B(M1)$  values, identify the regularities for them, and to predict some of the specific properties of heavy odd-odd nuclei along the  $N = Z$  line. Furthermore, taking into account very close relations of the Gamow-Teller transitions to M1 transitions, our results can be very helpful for the understanding of the quenching and fragmentation problems for Gamow-Teller  $\beta^+$  transitions, what was shown in our very recent paper [LiG01].

## List of Publications during PhD Project

My contributions to the results of scientific research performed at the Institut für Kernphysik der Universität zu Köln during my PhD Project are given in the following published papers:

- [LiL01] A. F. Lisetskiy, A. Gelberg, R. V. Jolos, N. Pietralla and P. von Brentano, *Quasideuteron states with deformed core*, Phys. Lett. B **512** (2001) 290.
- [LiN00] A. F. Lisetskiy, N. Pietralla, C. Fransen, R. V. Jolos and P. von Brentano, *Shell model description of "mixed-symmetry" states in  $^{94}\text{Mo}$* , Nucl. Phys. **A677** (2000) 100.
- [LiP99] A. F. Lisetskiy, R. V. Jolos, N. Pietralla and P. von Brentano, *Quasi-Deuteron Configurations in odd-odd  $N = Z$  nuclei*, Phys. Rev. **C60** (1999) 064310.
- [LiD01] A. F. Lisetskiy, C. Friessner, A. Schmidt, I. Schneider, N. Pietralla, P. von Brentano, R. V. Jolos, T. Otsuka, T. Sebe, Y. Utsuno, *Towards isovector  $M1$  transitions in odd-odd  $N = Z$  nuclei*, Proceedings of the International Conference "Nuclear Structure and Related Topics", (Dubna, Russia, June 6-10, 2000); *Yad.Fiz.* **64**, No 7, 1281 (2001); *Phys. At. Nucl.* **64**, 1206 (2001).
- [LiM01] A. F. Lisetskiy, A. Gelberg, N. Pietralla and P. von Brentano, *Collective Properties of odd-odd  $N = Z$  nuclei and Sum Rule for Isovector  $M1$  transitions*, Proceedings of the 7th International Spring Seminar on Nuclear Physics "Challenges of Nuclear Structure", Maiori, May 27-31, 2001; edited by A. Covello, World Scientific, Singapore, p.505 (2002).
- [LiG01] A. F. Lisetskiy, A. Gelberg, N. Pietralla and R. V. Jolos, *Influence of Quadrupole Deformation on Quasideuteron  $M1$  transitions in odd-odd  $N = Z$  nuclei*, Proceedings of the International Symposium on Nuclear Structure Physics, NP2001, Göttingen, March 5-8, 2001; World Scientific, Singapore, p. 377, (2001).
- [LiP00] A. F. Lisetskiy, C. Friessner, N. Pietralla, A. Schmidt, I. Schneider, P. von Brentano, R. V. Jolos, *Enhanced  $M1$  transitions and Collectivity in odd-odd  $N = Z$  Nuclei*, Proceedings of the NATO Advanced Study Institute "Nuclei far from Stability and Astrophysics", (Predeal, Romania, August 28 – September 8, 2000); Romanian Journal of Physics **46** (2001) 15 .

- [KIP01] H. Klein, A. F. Lisetskiy, N. Pietralla, C. Fransen, A. Gade, and P. von Brentano, *Proton-neutron mixed symmetry  $2_{ms}^+$  and  $3_{ms}^+$  states in  $^{96}\text{Ru}$* , Phys. Rev. C **65** (2002) 044315.
- [BrC01] P. von Brentano, A. F. Lisetskiy, C. Fransen, H. Klein, A. Gade, *Investigation of Properties of Mixed-Symmetry States in  $^{94}\text{Mo}$  and  $^{96}\text{Ru}$* , *The Nuclear Many-Body Problem 2001*, Proceedings of the NATO Advanced Research Workshop, Brijuni, Pula, Croatia, 2-5; W. Nazarewicz and D. Vretenar, Eds., Kluwer Academic Publishers, vol.53, (2002) 151.
- [BrE01] P. von Brentano, A. F. Lisetskiy, C. Friessner, N. Pietralla, A. Schmidt, I. Schneider, R. V. Jolos, *Approaching Rotational Collectivity in Odd-Odd  $N=Z$  Nuclei in  $pf$ -shell*, Prog. Part. Nucl. Phys. **46** (2001) 197.
- [BrM01] P. von Brentano, A. F. Lisetskiy, A. Dewald, C. Friessner, A. Schmidt, I. Schneider and N. Pietralla, *Quasideuteron configurations in  $^{46}\text{V}$  and  $^{58}\text{Cu}$* , Nucl. Phys. **A682** (2001) 48c.
- [ScC00] I. Schneider, A. F. Lisetskiy, C. Friessner, R. V. Jolos, N. Pietralla, A. Schmidt, D. Weisshaar, and P. von Brentano, *Low spin structure of the  $N=Z$  odd-odd nucleus  $^{54}_{27}\text{Co}_{27}$* , Phys. Rev. **C61** (2000) 044312.
- [BrE00] P. von Brentano, A. F. Lisetskiy, I. Schneider, C. Friessner, R. V. Jolos, N. Pietralla and A. Schmidt, *Low Spin Structure of Odd-Odd Nuclei*, Prog. Part. Nucl. Phys. **44** (2000) 29.
- [BrP00] P. von Brentano, A. F. Lisetskiy, C. Friessner, N. Pietralla, A. Schmidt, I. Schneider, R. V. Jolos, T. Otsuka, T. Sebe, Y. Utsuno, *Enhanced isovector  $M1$  transitions in odd-odd  $N = Z$  Nuclei in the  $pf$ -shell*, Proceedings of the International Workshop PINGST 2000 "Selected Topics on  $N=Z$  Nuclei", (Lund, Sweden, June 6-10, 2000), <http://pingst2000.kosufy.lu.se/proceedings/brentano.pdf>, p.170.
- [BrS99] P. von Brentano, A. F. Lisetskiy, I. Schneider, C. Friessner, R. V. Jolos, N. Pietralla and A. Schmidt, *Low Spin Spectroscopy of  $N=Z$  Nuclei: Quasi-Deuteron States in Odd-Odd Nuclei*, AIP Conference Proceedings **529** (2000) 58. (Capture Gamma-Ray Spectroscopy and Related Topics, 10<sup>th</sup> International Symposium, Edited by Stephen Wender; Santa Fe, New Mexico, 30 August - 3 September 1999); Melville, New York, 2000.

- [Fra01] C. Fransen, N. Pietralla, P. von Brentano, A. Dewald, J. Gableske, A. Gade, A. Lisetskiy and V. Werner, *First observation of a mixed-symmetry two- $Q$ -phonon  $2_{2,m_s}^+$  state in  $^{94}\text{Mo}$* , Phys. Lett. B **508** (2001) 219.
- [ScM00] A. Schmidt, I. Schneider, C. Friessner, A. F. Lisetskiy, N. Pietralla, T. Sebe, T. Otsuka, and P. von Brentano, *Low spin structure of the  $N=Z$  odd-odd nucleus  $^{50}_{25}\text{Mn}_{25}$* , Phys. Rev. **C62** (2000) 044319.
- [BrH00] P. von Brentano, C. Fransen, A. Gade, A. Lisetskiy and N. Pietralla, *Proton-Neutron Structure of Collective Excitations in  $^{94}\text{Mo}$* , Eur. Phys. J. A **13** (2002) 99.
- [BrB00] P. von Brentano, A. Dewald, C. Friessner, A. F. Lisetskiy, N. Pietralla, I. Schneider, A. Schmidt, T. Sebe, T. Otsuka, *Low-Spin Spectroscopy of  $^{50}\text{Mn}$* , Proceedings of the "Bologna 2000 - Structure of the Nucleus at the Dawn of the Century" Conference, (Bologna, Italy, May 29 - June 3, 2000); e-preprint: nucl-th 0009043.
- [PiT00] N. Pietralla, C. Fransen, A. F. Lisetskiy, P. von Brentano, *Multiphonon mixed-symmetry states accessible to the shell model*, Proceedings of the RIKEN Symposium "Shell Model 2000", (Riken, Japan, 5-8 March, 2000); *Nucl. Phys.* **A704** (2002) 69.
- [BrT00] P. von Brentano, A. Schmidt, I. Schneider, C. Friessner, A. F. Lisetskiy, N. Pietralla, R. V. Jolos, T. Sebe, T. Otsuka, *Low-Spin Structure of odd-odd  $N = Z$  Nuclei  $^{54}\text{Co}$  and  $^{50}\text{Mn}$* , Proceedings of the RIKEN Symposium "Shell Model 2000", (Riken, Japan, 5-8 March, 2000); *Nucl. Phys.* **A704**, (2002) 115.
- [BrR99] P. von Brentano, A. Dewald, C. Fransen, C. Friessner, R. V. Jolos, A. F. Lisetskiy, N. Pietralla, I. Schneider, A. Schmidt, *Isospin and  $F$ -spin changing  $M1$  transitions in Nuclei*, Proc. Intern. Symposium Advances in Nuclear Physics, Bucharest, Romania, 9-10 December, 1999, D. Poenaru, S. Stoica, Eds., World Scientific, Singapore, p. 265 (2000).
- [PiY01] N. Pietralla, R. Krücken, C. J. Barton, C. W. Beausang, M. A. Caprio, R. F. Casten, J. R. Cooper, A. A. Hecht, J. R. Novak, N. V. Zamfir, A. Lisetskiy, and A. Schmidt, *Lifetimes of quasideuteron configurations in the odd-odd  $N = Z$  nucleus  $^{50}_{25}\text{Mn}_{25}$* , Phys. Rev. **C65** (2002) 024317.



# Bibliography

- [Ari75] A. Arima, and F. Iachello, *Phys. Rev. Lett.* 35 (1975) 1069 .
- [Ari77] A. Arima, T. Otsuka, F. Iachello, and I. Talmi, *Phys. Rev. Lett.* 66 (1977) 205 .
- [Asc68] R. J. Ascutto, D. A. Bell and J. P. Davidson, *Phys. Rev. C* 176 (1968) 1323 .
- [Bal94] G. Baldsiefen, H. Hubel, W. Korten, D. Mehta, N. Nenoff, B. V. T. Rao, P. Willsau, H. Grawe, J. Heese, H. Kluge, K. H. Maier, R. Schubart, S. Frauendorf, H. J. Maier, *Nucl. Phys. A* 574 (1994) 521 .
- [Bar32] J.H. Bartlett, *Phys. Rev.* 41 (1932) 370.
- [Bog57] N. N. Bogolubov, *Dokl. Akad. Nauk SSSR* 119 (1958) 52.
- [Boh53] A. Bohr, and B. R. Mottelson, *Dan. Vid. Selsk., Mat.-Fys. Medd.* No.16 (1953).
- [Boh69] A. Bohr and B. R. Mottelson, *Nuclear Structure*, vol.II, (Benjamin: New York, 1969).
- [Bra96] F. Brandolini, M. Ionescu-Bujor, N. H. Medina, R. V. Ribas, D. Bazzacco, M. De Poli, P. Pavan, C. Rossi Alvarez, G. de Angelis, S. Lunardi, D. De Acuna, D. R. Napoli, S. Frauendorf, *Phys. Lett. B* 388 (1996) 468 .
- [BrE00] P. von Brentano, A. F. Lisetskiy, I. Schneider, C. Friessner, R. V. Jolos, N. Pietralla and A. Schmidt, *Prog. Part. Nucl. Phys.* 44 (2000) 29 .
- [BrB00] P. von Brentano, A. Dewald, C. Friessner, A. F. Lisetskiy, N. Pietralla, I. Schneider, A. Schmidt, T. Sebe, T. Otsuka, *Proceedings of the "Bologna*

2000 - Structure of the Nucleus at the Dawn of the Century” Conference, Bologna, Italy, May 29 - June 3, 2000, preprint nucl-th/0009043.

- [BrM01] P. von Brentano, A. F. Lisetskiy, A. Dewald, C. Friessner, A. Schmidt, I. Schneider and N. Pietralla, *Nucl. Phys. A* 682 (2001) 48c .
- [BrE01] P. von Brentano, A. F. Lisetskiy, C. Friessner, N. Pietralla, A. Schmidt, I. Schneider, R. V. Jolos, *Prog. Part. Nucl. Phys.* 46 (2001) 197 .
- [Bri98] J. Britz, A. Pape, and M. S. Antony, *At. Data Nucl. Data Tables* 69 (1998) 125.
- [Bru77] P. J. Brussaard and P. W. M. Glaudemans, *Shell-model applications in nuclear spectroscopy*, (North-Holland Publishing Company, Amsterdam, 1977).
- [Car99] E. Caurier, G. Matrinez-Pinedo, F. Nowacki, A. Poves, J. Retamosa, A. P. Zuker, *Phys. Rev. C* 55 (1997) 187 .
- [Cho91] W.-T. Chou, J.-Y. Zhang, R.F. Casten, and D.S. Brenner, *Phys. Lett. B* 255 (1991) 487.
- [Cla93] R. M. Clark, R. Wadsworth, E. S. Paul, C. W. Beausang, I. Ali, A. Astier, D. M. Cullen, P. J. Dagnall, P. Fallon, M.J. Joyce, M. Meyer, N. Redon, P. H. Regan, J. F. Sharpey-Schafer, W. Nazarewicz, R. Wyss, *Nucl. Phys. A* 562 (1993) 121
- [Cla97] R. M. Clark, S. J. Asztalos, G. Balzsiefen, J. A. Becker, L. Bernstein, M. A. Deleplanque, R. M. Diamond, P. Fallon, I. M. Hibbert, H. Hubel, R. Krucken, I. Y. Lee, A. O. Macchiavelli, R. W. MacLeod, G. Schmid, F. S. Stephens, K. Vetter, R. Wadsworth, S. Frauendorf, *Phys. Rev. Lett.* 78 (1997) 1868 .
- [Cla98] R. M. Clark, R. Krucken, S. J. Asztalos, J. A. Becker, B. Busse, S. Chmel, M. A. Deleplanque, R. M. Diamond, P. Fallon, D. Jenkins, K. Hauschild, I. M. Hibbert, H. Hubel, I. Y. Lee, A. O. Macchiavelli, R. W. MacLeod, G. Schmid, F. S. Stephens, U. J. van Severen, K. Vetter, R. Wadsworth, S. Wan, *Phys. Lett. B* 440 (1998) 251 .
- [Dav58] A. S. Davydov and G. F. Filippov, *Nucl. Phys.*, 8 (1958) 237.

- [Dra83] J. P. Draayer, and K. J. Weeks, *Phys. Rev. Lett.* 16 (1983) 1422 .
- [Duk01] J. Dukelsky, S. Pittel, *Phys. Rev. C* 63 (2001) 061303 .
- [Els33] W. M. Elsasser, *J. de Phys. et Rad.*, 4 (1933) 549.
- [Els35] W. M. Elsasser, *J. de Phys. et Rad.* 6 (1935) 473.
- [Ell58] J. P. Elliott, *Proc. Roy. Soc.* 245 (1958) 128.
- [End93] P. M. Endt, *At. Data Nucl. Data Tables* 55 (1993) 171.
- [Fra93] S. Frauendorf, *Nucl. Phys. A* 557 (1993) 259c .
- [Fri99] C. Friessner, N. Pietralla, A. Schmidt, I. Schneider, Y. Utsuno, T. Otsuka, and P. von Brentano, *Phys. Rev. C* 60 (1999) 011304 .
- [Fri00] C. Friessner, *Ph.D. thesis*, (Univerität zu Köln, 2000).
- [Gad97] A. Gadea, G. de Angelis, C. Fahlander, M. De Poli, E. Farnea, Y. Li, D. R. Napoli, Q. Pan, P. Spolaore, D. Bazzacco, S. M. Lenzi, S. Lunardi, C. M. Petrache, F. Brandolini, P. Pavan, C. Rossi Alvarez, M. Sferrazza, P. G. Bizzeti, A. M. Bizzeti Sona, J. Nyberg, M. Lipoglavsek, J. Persson, J. Cederkall, D. Seweryniak, A. Johnson, H. Grawe, F. Soramel, M. Ogawa, A. Makishima, R. Schubart, S. Frauendorf, *Phys. Rev. C* 55 (1997) R1 .
- [Goo98] A. L. Goodman, *Phys. Rev. C* 58 (1998) R3051 .
- [Gui98] H. de Guise, D. J. Rowe, *Nucl. Phys. A* 636 (1998) 47.
- [Hax49] O. Haxel, J. H. D. Jensen and H. E. Suess, *Phys. Rev.* 75 (1949) 1766.
- [Hei32] W. Heizenberg, *Z. Phys.* 77 (1932) 1.
- [Hey94] K. L. G. Heyde, *The Nuclear Shell Model*, (Springer-Verlag, Berlin Heidelberg, 1994).
- [Irv72] J. M. Irvine, *Nuclear Structure Theory*, (Pergamon Press: Oxford, 1972).
- [Isa97] P. Van Isacker, and D. D. Warner, *Phys. Rev. Lett.* 78 (1997) 3266 .
- [Iwa32] D. D. Iwanenko, *Nature* 129 (1932) 798.
- [Jan74] D. Janssen, R. V. Jolos, and F. Dönau, *Nucl. Phys. A* 224 (1974) 93 .

- [Jen98] D. G. Jenkins, I. M. Hibbert, C. M. Parry, R. Wadsworth, D. B. Fossan, G. J. Lane, J. M. Sears, J. F. Smith, R. M. Clark, R. Krucken, I. Y. Lee, A. O. Macchiavelli, V. P. Janzen, J. Cameron, S. Frauendorf, *Phys. Lett. B* 428 (1998) 23 .
- [Jen99] D. G. Jenkins, R. Wadsworth, J. A. Cameron, R. M. Clark, D. B. Fossan, I. M. Hibbert, V. P. Janzen, R. Krucken, G. J. Lane, I. Y. Lee, A. O. Macchiavelli, C. M. Parry, J. M. Sears, J. F. Smith, S. Frauendorf, *Phys. Rev. Lett.* 83 (1999) 500 .
- [Jol75] R. V. Jolos, F. Dönau, and D. Janssen, *Yad. Fiz.* 22 (1975) 965.
- [Ker61] A. K. Kerman, *Ann. Phys.* 12 (1961) 300.
- [Lan97] K. Langanke, D. J. Dean, S. E. Koonin, P. B. Radha, *Nucl. Phys. A* 613 (1997) 253.
- [Len99] S.M. Lenzi, D. R. Napoli, C. A. Ur, D. Bazzacco, F. Brandolini, J. A. Cameron, E. Caurier, G. de Angelis, M. De Poli, E. Farnea, A. Gadea, S. Hankonen, S. Lunardi, G. Martinez-Pinedo, Zs. Podolyak, A. Poves, C. Rossi Alvarez, J. Sanchez Solano, H. Somacal, *Phys. Rev. C* 60 (1999) 021303 .
- [LiG01] A. F. Lisetskiy, A. Gelberg, N. Pietralla and R. V. Jolos, *Proceedings of the International Symposium on Nuclear Structure Physics*, NP2001, Göttingen, March 5-8, 2001; World Scientific, Singapore, p. 377, (2001).
- [LiP99] A. F. Lisetskiy, R. V. Jolos, N. Pietralla, and P. von Brentano, *Phys. Rev. C* 60 (1999) 064310 .
- [LiL01] A. F. Lisetskiy, A. Gelberg, R. V. Jolos, N. Pietralla, P. von Brentano, *Phys. Lett. B* 512 (2001) 290 .
- [Mac98] A. O. Macchiavelli, R. M. Clark, P. Fallon, M. A. Deleplanque, R. M. Diamond, R. Krucken, I. Y. Lee, F. S. Stephens, S. Asztalos, K. Vetter, *Phys. Rev. C* 57 (1998) R1073 .
- [Mac00] A. O. Macchiavelli, P. Fallon, R. M. Clark, M. Cromaz, M. A. Deleplanque, R. M. Diamond, G. J. Lane, I. Y. Lee, F. S. Stephens, C. E. Svensson, K. Vetter, D. Ward, *Phys. Rev. C* 61 (2000) 041303 .

- [MaC00] A. O. Macchiavelli, P. Fallon, R. M. Clark, M. Cromaz, M. A. Deleplanque, R. M. Diamond, G. J. Lane, I. Y. Lee, F. S. Stephens, C. E. Svensson, K. Vetter, D. Ward *Phys. Lett. B* **480**, 1 (2000).
- [Mar97] G. Matrinez-Pinedo, A. P. Zuker, A. Poves, and E. Caurier, *Phys. Rev. C* **55** (1997) 187 .
- [May49] M. Göppert-Mayer, *Phys. Rev.* **75** (1949) 1969.
- [May55] M. Göppert-Mayer and J. H. D. Jensen, *Elementary Theory of Nuclear Shell Structure*, (Wiley, New York, 1955).
- [Mos84] M. Moshinsky, *J. Math. Phys.* **25** (1984) 1555.
- [Naz99] W. Nazarewicz, *Nucl. Phys. A* **654** (1999) 195c .
- [Nil55] S. G. Nilsson, *Mat. Fys. Medd. Dan. Vid. Selsk.*, **29** (1955) n.16 .
- [OLe99] C.D. O’Leary, M. A. Bentley, D. E. Appelbe, R. A. Bark, D. M. Cullen, S. Erturk, A. Maj, J. A. Sheikh, D. D. Warner, *Phys. Lett. B* **459** (1999) 73 .
- [Ots98] T. Otsuka, M. Honma, and T. Mizusaki, *Phys. Rev. Lett.* **81** (1998) 1588 .
- [Ots01] T. Otsuka, R. Fujimoto, Y. Utsuno, B. A. Brown, M. Honma, T. Mizusaki, *Phys. Rev. Lett.* **87** (2001) 082502 .
- [Pet99] A. Petrovici, K.W. Schmid, A. Faessler, *Nucl. Phys. A* **647** (1999) 197 .
- [PiY01] N. Pietralla, R. Krücken, C. J. Barton, C. W. Beausang, M. A. Caprio, R. F. Casten, J. R. Cooper, A. A. Hecht, J. R. Novak, N. V. Zamfir, A. Lisetskiy, and A. Schmidt, *Phys. Rev. C* (2001) in press .
- [Pla66] A. Plastino, R. Arvieu, S.A. Moszkowski, *Phys. Rev.* **145** (1966) 837.
- [Pov98] A. Poves, and G. Martinez-Pinedo, *Phys. Lett. B* **430** (1998) 203 .
- [Rat73] R. D. Ratna Raju, J. P. Draayer, and K. T. Hecht, *Nucl. Phys. A* **202** (1973) 433 .
- [Row85] D. J. Rowe, *Rep. Prog. Phys.* **48** (1985) 1419.

- [Rud96] D. Rudolph, C.J. Gross, J.A. Sheikh, D.D. Warner, I.G. Bearden, R.A. Cunningham, D. Foltescu, W. Gelletly, F. Hannachi, A. Harder, T.D. Johnson, A. Jungclaus, M.K. Kabadiyski, D. Kast, K.P. Lieb, H.A. Roth, T. Shizuma, J. Simpson, Ö. Skeppstedt, B.J. Varley, and M. Weiszflog, *Phys. Rev. Lett.* 76 (1996) 376 .
- [Rud98] D. Rudolph C. Baktash, W. Satula, J. Dobaczewski, W. Nazarewicz, M. J. Brinkman, M. Devlin, H.-Q. Jin, D. R. LaFosse, L. L. Riedinger, D. G. Sarantites, C.-H. Yu, *Nucl. Phys. A* 630 (1998) 417c .
- [Sat97] W. Satula, and R. Wyss, *Phys. Lett. B* 393 (1997) 1.
- [Sat98] W. Satula, J. Dobaczewski, and W. Nazarewicz, *Phys. Rev. Lett.* 81 (1998) 3599.
- [ScM00] A. Schmidt, I. Schneider, C. Friessner, A. F. Lisetskiy, N. Pietralla, T. Sebe, T. Otsuka, and P. von Brentano, *Phys. Rev. C* 62 (2000) 044319 .
- [ScC99] I. Schneider, A. F. Lisetskiy, C. Friessner, R. V. Jolos, N. Pietralla, A. Schmidt, D. Weisshaar, and P. von Brentano, *Phys. Rev. C* 61 (2000) 0444312 .
- [Sch00] I. Schneider, *Ph.D. thesis*, (Universität zu Köln, 2000).
- [Sko98] S. Skoda, B. Fiedler, F. Becker, J. Eberth, S. Freund, T. Steinhardt, O. Stuch, O. Thelen, H.G. Thomas, L. Käubler, J. Reif, H. Schnare, R. Schwengner, T. Servene, G. Winter, V. Fischer, A. Jungclaus, D. Kast, K.P. Lieb, C. Teich, C. Ender, T. Härtlein, F. Kock, D. Schwalm, and P. Baumann, *Phys. Rev. C* 58 (1998) R5 .
- [Sve98] C.E. Svensson, S.M. Lenzi, D.R. Napoli, A. Poves, C.A. Ur, D. Bazzacco, F. Brandolini, J.A. Cameron, G. de Angelis, A. Gadea, D.S. Haslip, S. Lunardi, E.E. Maqueda, G. Martínez-Pinedo, M.A. Nagarajan, C. Rossi Alvarez, A. Vitturi, and J.C. Waddington, *Phys. Rev. C* 58 (1998) R2621 .
- [Tal93] I. Talmi, *Simple Models of Complex Nuclei*, (Harwood Academic Publishers GmbH, Chur, Switzerland, 1993).
- [Var99] C. Vargas, J. G. Hirsch, P. O. Hess, J. P. Draayer, *Phys. Rev. C* 58 (1998) 1488 .

- [Vin98] S.M. Vincent, P.H. Regan, D.D. Warner, R.A. Bark, D. Blumenthal, M.P. Carpenter, C.N. Davids, W. Gelletly, R.V.F. Janssens, C.D. O'Leary, C.J. Lister, J. Simpson, D. Seweryniak, T. Saitoh, J. Schwartz, S. Törmänen, O. Juillet, F. Nowacki, and P. Van Isacker, *Phys. Lett. B* 437 (1998) 264 .
- [Vog00] P. Vogel, *Nucl. Phys. A* 662 (2000) 148 .
- [Was71] P. Wasilewski and F. B. Malik, *Nucl. Phys. A* 160 (1971) 113 .
- [Zam88] L. Zamick, D.C.Zheng, *Phys. Rev. C* 37 (1988) 1675 .
- [Zam99] L. Zamick, N. Auerbach, *Nucl. Phys. A* 658 (1999) 258 .
- [Zuk95] A. P. Zuker, J.Retamosa, A. Poves, and E. Caurier, *Phys. Rev. C* 52 (1995) R1741 .

# Acknowledgments

First of all I want to thank Professor Peter von Brentano for his close and patient supervisorship, for many interesting ideas, mental impulses and unusual thought-provoking questions that have strengthened my curiosity and interest in physics, deepened my understanding of nuclear phenomena, and significantly broadened my scope. I am very grateful him for warm care of me and my family.

I have strongly benefited from creative and friendly atmosphere at the Institute for Nuclear Physics and I would like to thank all the members and guests of the Institute for this. I express my special thanks and gratitude to the following:

Prof. Dr. A. Gelberg, Dr. N. Pietralla, Prof. Dr. R.V. Jolos, Dr. I. Schneider, Dr. C. Friessner, Dr. A. Schmidt, and Dr. C. Fransen for many fruitful discussions and close collaboration;

Dr. L. Esser and Dr. F. Becker for the introduction to the world of shell model codes I have used during my work at the Institute;

Dr. H. Klein and Dr. R. Peusquens for a lot of consultations on the operation system and software problems I have faced;

Dr. A. Zilges who has helped me to establish contacts with the Institute and to come here;

DAAD for the financial support of my researches during the first year of my stay at the Institute;

Prof. Dr. A. Gelberg, Dr. H. Klein, Dipl.-Phys. K. Jessen and Dipl.-Phys. V. Werner for careful reading of the manuscript, valuable comments and corrections;

Prof. Dr. G. F. Filippov and Prof. Dr. I. S. Dotsenko, who taught me to operate analytical methods of nuclear theory during the time of my studies in Kiev;

Dr. G. Pascovici, A. Wedel, Dr. N. Pietralla, and Dr. R.-D. Herzberg for the help with my settlement problems in Cologne and a number of useful advises;

Dr. K.O.Zell for the help in the fighting with the wall of bureaucratic formalities;

My wife, Oksana, and son, Vladik, for their patience, understanding and moral support;

My parents and parents in law for moral support, for pleasant summer vacation time we spent together in Tatarbunary, on Black Sea coast and in Komsomolsk, on Dnipro river, during the last few years.



## **Erklärung**

Ich versichere, daß ich die von mir vorgelegte Dissertation selbständig angefertigt, die benutzten Quellen und Hilfsmittel vollständig angegeben und die Stellen der Arbeit - einschließlich Tabellen, Karten und Abbildungen -, die anderen Werken im Wortlaut oder dem Sinn nach entnommen sind, in jedem Einzelfall als Entlehnung kenntlich gemacht habe; daß diese Dissertation noch keiner anderen Fakultät oder Universität zur Prüfung vorgelegen hat; daß sie abgesehen von unten angegebenen Teilpublikationen noch nicht veröffentlicht worden ist sowie, daß ich eine solche Veröffentlichung vor Abschluß des Promotionsverfahrens nicht vornehmen werde. Die Bestimmungen dieser Promotionsordnung sind mir bekannt. Die von mir vorgelegte Dissertation ist von Professor Dr. P. von Brentano betreut worden.

Bereits publiziert sind Teile aus den Kapiteln 2 und 3 in [LiP99, LiL01, ScC99, BrE01].

# Lebenslauf

Name: Alexander Federovytsch Lisetskiy  
Geburtsdatum: 04.06.1972  
Geburtsort: Tatarbunary, Ukraine  
Staatsangehörigkeit: ukrainisch  
Mutter: Lidiya Pylypivna Lisetska, geb. Tschumatschenko  
Vater: Fedir Ivanovytsch Lisetskiy  
Ehefrau: Oksana Bogdanivna Lisetska, geb. Wojtowysch  
Kind: Vladyslav Lisetskiy

## Schulbildung:

Sep. 1979 – Jun. 1982 Grundschule 1, Tatarbunary, Ukraine  
Sep. 1982 – Jun. 1989 Schule 1, Tatarbunary, Ukraine

## Hochschulstudium:

Sep. 1989 – Jun. 1994 Studium an der Fakultät für Physik der  
Kiew Taras Schewtschenko Universität  
Juni 1994 Diplom im Fach Physik mit dem Thema:  
"Mikroskopisches Kernmodell von zwei  
axialsymmetrischen Kreiseln"  
Seit Juli 1998 Promotionsstudium

## Arbeitsverhältnisse:

### an der Fakultät für Physik der Kiew Universität, Ukraine

Nov. 1994 – Sep. 1997 Forschungsassistent, Abteilung Quanten Feld Theorie

### am Institut für Kernphysik der Universität zu Köln:

Seit Oktober 1997 - Wissenschaftlicher Mitarbeiter

## Stipendium:

Okt. 1997 – Jul. 1998 DAAD Stipendium (Studium ohne Abschluss).

**Adresse:** Lindenthalgürtel 74, 50935 Köln